DOI: 10.1002/chem.200500857

Polynuclear Bismuth-Oxo Clusters: Insight into the Formation Process of a Metal Oxide

Michael Mehring,* Dirk Mansfeld, Sanna Paalasmaa, and Markus Schürmann[a]

Abstract: The reaction of the bismuth silanolates $[Bi(OSiR_2R')_3]$ (R = R′ = Me, Et, *i*Pr; R = Me, R′ = *t*Bu) with water has been studied. Partial hydrolysis gave polynuclear bismuth-oxo clusters whereas amorphous bismuth-oxo(hydroxy) silanolates were obtained when an excess of water was used in the hydrolysis reaction. The metathesis reaction of $BiCl_3$ with $NaOSiMe_3$ provided mixtures of heterobimetallic silanolates. The molecular structures of $[Bi_{18}Na_4O_{20}(OSiMe_3)_{18}]$ (**2**), $[Bi_{33}NaO_{38}(OSiMe_3)_{24}]\cdot 3C_7H_8$ (**3**·3 C_7H_8), $[Bi_{50}Na_2O_{64}(OH)_2(OSiMe_3)_{22}]\cdot 2C_7H_8\cdot 2H_2O$ (**4**·2 C_7H_8·2 H_2O), $[Bi_4O_2(OSiEt_3)_8]$ (**5**), $[Bi_9O_7(OSiMe_3)_{13}]\cdot 0.5C_7H_8$ (**6**·0.5 C_7H_8), $[Bi_{18}O_{18}(OSiMe_3)_{18}]\cdot 2C_7H_8$ (**7**·2 C_7H_8) and $[Bi_{20}O_{18}(OSiMe_3)_{24}]\cdot 3C_7H_8$ (**8**·3 C_7H_8) are presented and compared with the solid-state structures of $[Bi_{22}O_{26}(OSiMe_2tBu)_{14}]$ (**9**) and β-Bi_2O_3. Compound **2** crystallises in the triclinic space group $P\bar{1}$ with the lattice constants a = 17.0337(9), b = 19.5750(14), c = 26.6799(16) Å, α = 72.691(4), β = 73.113(4) and γ = 70.985(4)°; compound **3**·3 C_7H_8 crystallises in the monoclinic space group $P2_1/n$ with the lattice constants a = 20.488(4), b = 22.539(5), c = 26.154(5) Å and β = 100.79(3)°; compound **4**·2 C_7H_8·2 H_2O crystallises in the monoclinic space group $P2_1/n$ with the lattice constants a = 20.0518(12), b = 24.1010(15), c = 27.4976(14) Å and β = 103.973(3)°; compound **5** crystallises in the monoclinic space group $P2_1/c$ with the lattice constants a = 25.256(5), b = 15.372(3), c = 21.306(4) Å and β = 113.96(3)°; compound **6**·0.5 C_7H_8 crystallises in the triclinic space group $P\bar{1}$ with the lattice constants a = 15.1916(9), b = 15.2439(13), c = 22.487(5) Å, α = 79.686(3), β = 74.540(5) and γ = 66.020(4)°; compound **7**·2 C_7H_8 crystallises in the triclinic space group $P\bar{1}$ with the lattice constants a = 14.8295(12), b = 16.1523(13), c = 18.4166(17) Å, α = 75.960(4), β = 79.112(4) and γ = 63.789(4)°; and compound **8**·3 C_7H_8 crystallises in the triclinic space group $P\bar{1}$ with the lattice constants a = 17.2915(14), b = 18.383(2), c = 18.4014(18) Å, α = 95.120(5), β = 115.995(5) and γ = 106.813(5)°. The molecular structures of the bismuth-rich compounds are related to the CaF_2-type structure. Formally, the hexanuclear $[Bi_6O_8]^{2+}$ fragment might be described as the central building unit, which is composed of bismuth atoms placed at the vertices of an octahedron and oxygen atoms capping the trigonal faces. Depending on the reaction conditions and the identity of R, the thermal decomposition of the hydrolysis products $[Bi_nO_l(OH)_m(OSiR_3)_{3n-(2l-m)}]$ gives α-Bi_2O_3, β-Bi_2O_3, $Bi_{12}SiO_{20}$ or $Bi_4Si_3O_{12}$.

Keywords: bismuth · cluster compounds · crystal structures · metal oxides · silanolates

Introduction

Heterometallic bismuth oxide based materials have found widespread applications as catalysts, nontoxic pigments, oxide ion conductors, superconductors, gas sensors and ferroelectric or piezoelectric devices. Among the heterometallic oxides, a variety of combinations such as Bi/Ti/O,[1–3] Bi/Nb/O,[4] Bi/Sr/Ta/O,[5] Bi/Mo/O,[6,7] Bi/V/O[8,9] and Bi/Fe/O[10] have been extensively studied. Four polymorphs of the binary metal oxide Bi_2O_3 (α, β, γ and δ phases) have been reported[11,12] and are of growing interest with respect to the synthesis of novel nanoscale devices. Initially, it was mainly the optical and electrical properties of bismuth oxide thin films that were investigated,[13,14] but recent studies have focussed on nanoparticles[15] and nanowires.[16] Although chemical vapour deposition techniques have been used for the synthesis of homo- and heterometallic bismuth oxide

[a] Dr. M. Mehring, D. Mansfeld, S. Paalasmaa, Dr. M. Schürmann
Anorganische Chemie II
Fachbereich Chemie der Universität Dortmund
Otto-Hahn-Str. 6, 44227 Dortmund (Germany)
Fax: (+49) 231-755-5048
E-mail: michael.mehring@uni-dortmund.de

Supporting information for this article is available on the WWW under http://www.chemeurj.org/ or from the author.

films,[2,14,17,18] wet chemical approaches towards bismuth-containing materials such as the sol–gel process have found broader application.[3,9,19,20] The sol–gel process offers several advantages, such as mild processing temperatures and aggregation of molecular precursors in solution prior to formation of the final material. This approach gives access to thermodynamically stable as well as metastable compounds and favours the formation of homogeneous products. The high potential of single-source precursors has motivated several research groups to investigate the reactivity and the structural chemistry of heterometallic bismuth precursors in order to obtain more information on how to control the composition and morphology of the final material at the molecular level.[4,7,20–26] Following this strategy, simple bismuth alkoxides, which have been reported previously but have not attracted considerable interest until recently,[17,25,27–29] represent potential starting materials for heterometallic single-source precursors such as $[BiTi_2(\mu_3\text{-}O)(\mu_3\text{-}O\textit{i}Pr)_4(O\textit{i}Pr)_5]$.[30] Alkoxide ligands at the periphery of the metal-oxo alkoxides offer the potential for further aggregation through hydrolysis/condensation reactions. However, the hydrolysis process of metal alkoxides is difficult to control and often leads to the intimate formation of intractable solids. This is especially pronounced in the case of heavy main group metals. Large organic substituents reduce the reactivity, but often to an extent which reduces the potential application of these alkoxides as precursors for the sol–gel process. As a result of steric constraints, polynuclear bismuth-oxo alkoxides such as $[Bi_8(\mu_4\text{-}O)_2(\mu_3\text{-}O)_2(\mu\text{-}OC_6F_5)_{16}]$[23] and $[Bi_9(\mu_3\text{-}O)_7(\mu_3\text{-}OR)(OR)_{12}]$ (R = C_6F_5, 2,6-$C_6H_3Cl_2$)[23,31,32] are among the largest bismuth-oxo alkoxides reported to date and the formation of larger aggregates with sterically hindered ligands seems unlikely. Addition of auxiliary ligands is one strategy towards larger multimetallic compounds such as $[Bi_8Ti_8(sal)_{20}(\mu\text{-}O\textit{i}Pr)_8(O\textit{i}Pr)_8]$ (sal = salicylate),[24] which also show a reduced reactivity of the metal alkoxide bonds.[21] Similarly, replacing alkoxides by silanolate ligands might be expected to slow down the hydrolysis reaction and reduce the tendency for aggregation through intermolecular M···OR bonds to give poorly soluble coordination polymers.[33]

However, reports on bismuth silanolates are restricted to a few compounds and most studies have focussed on synthetic aspects. Four different synthetic routes have been established for bismuth silanolates such as $[Bi(OSiR_3)_3]$ (R = Me,[34,35] Et,[35] *i*Pr,[35] Ph,[36] O*t*Bu[37]) and $[Bi(OSiR_2R')_3]$ (R = O*t*Bu, R′ = Ph;[37] R = Me, R′ = *t*Bu;[38] R = Ph, R′ = *t*Bu[39]) (Scheme 1).

We are interested in the formation process of bismuth oxide starting from molecular precursors and have initiated studies on the hydrolysis process of bismuth silanolates. A thorough understanding of this process might provide information on how to control the composition and morphology of homo- and heterometallic bismuth-containing materials produced by way of wet chemical processes. Partial hydrolysis of $[Bi(OSiMe_2tBu)_3]$ was reported to give the polynuclear bismuth-oxo cluster $[Bi_{22}O_{26}(OSiMe_2tBu)_{14}]$,[38] and here we report an extension of this study on the hydrolysis process concerning $[Bi(OSiR_3)_3]$ (R = Me, Et, *i*Pr).[35] Single-crystal X-ray structure analyses of the bismuth-oxo clusters $[Bi_{18}Na_4O_{20}(OSiMe_3)_{18}]$ (**2**), $[Bi_{33}NaO_{38}(OSiMe_3)_{24}]$ (**3**), $[Bi_{50}Na_2O_{64}(OH)_2(OSiMe_3)_{22}]$ (**4**), $[Bi_4O_2(OSiEt_3)_8]$ (**5**), $[Bi_9O_7(OSiMe_3)_{13}]$ (**6**), $[Bi_{18}O_{18}(OSiMe_3)_{18}]$ (**7**) and $[Bi_{20}O_{18}(OSiMe_3)_{24}]$ (**8**) are reported, and their structural relationships with $[Bi_{22}O_{26}(OSiMe_2tBu)_{14}]$ (**9**)[38] and β-Bi_2O_3 are discussed.

$$[Bi\{N(SiMe_3)_2\}_3] + 3\,R_3SiOH \xrightarrow[-\,3\,HN(SiMe_3)_2]{} [Bi(OSiR_3)_3] \quad R = Ph \qquad (1)$$

$$[Bi(OtBu)_3] + 3\,R_2R'SiOH \xrightarrow[-\,3\,tBuOH]{} [Bi(OSiR_2R')_3] \quad R = R' = Me, Et, iPr, OtBu;\ R = Me, Ph, R' = tBu;\ R = OtBu, R' = Ph \qquad (2)$$

$$BiPh_3 + 3\,R_2R'SiOH \xrightarrow[-\,3\,C_6H_6]{} [Bi(OSiR_2R')_3] \quad R = Ph,\ R' = tBu \qquad (3)$$

$$BiCl_3 + 3\,NaOSiR_3 \xrightarrow[-\,3\,NaCl]{} [Bi(OSiR_3)_3] \quad R = Me, OtBu \qquad (4)$$

Scheme 1. The synthetic routes that have been established for bismuth silanolates.

Results

Initially, we tried to synthesise $[Bi(OSiMe_3)_3]$ by a metathesis reaction starting from $MOSiMe_3$ (M = Li, Na, K) and $BiCl_3$ according to Equation (4). For M = Li, K, ill-defined and poorly soluble solids were obtained and for M = Na heterometallic bismuth-oxo clusters were produced. We have recently reported that heating a mixture of $BiCl_3$ and $NaOSiMe_3$ gave the heterometallic bismuth-oxo silanolate $[Bi_2Na_4O(OSiMe_3)_8]$ (**1**) and $Me_3SiOSiMe_3$. In the presence of air moisture, the heterometallic bismuth-oxo clusters $[Bi_{10}Na_5O_7(OH)_6(OSiMe_3)_{15}]$ and $[Bi_{15}Na_3O_{18}(OSiMe_3)_{12}]$ were obtained.[40] It appeared likely that the metathesis reaction at ambient or low temperature and under rigorous exclusion of moisture might give access to $[Bi(OSiMe_3)_3]$. However, reaction of $BiCl_3$ with $NaOSiMe_3$ at room temperature also gave $Me_3SiOSiMe_3$, which is indicative of the formation of bismuth-oxo clusters. Crystallisation from toluene/benzene gave a large quantity of highly moisture-sensitive single crystals. The crystalline fraction appeared to be heterogeneous by visual inspection under a microscope, which was confirmed by X-ray diffraction analyses of several single crystals. We identified $[Bi_2Na_4O(OSiMe_3)_8]$ (**1**) as the major product, and $[Bi_{18}Na_4O_{20}(OSiMe_3)_{18}]$ (**2**) and $[Bi_{33}NaO_{38}(OSiMe_3)_{24}]$ (**3**) as byproducts. Single crystals of compound **2** were also isolated by crystallisation from pentane. In a similar experiment but with prolonged storage at 0 °C, we observed a mixture composed of compound **1** as the major product and $[Bi_{50}Na_2O_{64}(OH)_2(OSiMe_3)_{22}]$ (**4**) as a minor product (Scheme 2). The identities of both were con-

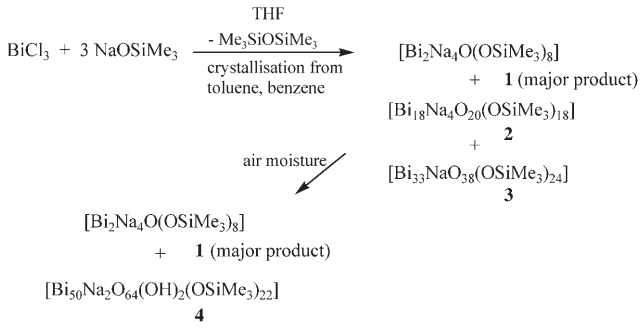

Scheme 2. The synthetic route used to obtain compounds **1**–**4**.

firmed by single-crystal X-ray diffraction analyses. Apparently, the heterometallic oxo cluster **4** is a hydrolysis product of the initially formed compounds. The molecular structures of compounds **3** and **4** reveal remarkable insight into the formation process of Bi_2O_3 and are thus discussed here, together with the homometallic bismuth-oxo clusters (see below).

As our attempts to prepare $[Bi(OSiMe_3)_3]$ from the metathesis route failed, alkoxide-silanol exchange was used to prepare the homoleptic bismuth silanolates $[Bi(OSiR_2R')_3]$ (R = R′ = Me, Et, *i*Pr; R = Me, R′ = *t*Bu) [Eq. (2)].

It is well known that the hydrolysis of metal silanolates $[M(OSiR_3)_z]_n$ proceeds by the formation of small aggregates of metal-oxo(hydroxy) siloxides, which are further linked by hydrolysis-condensation reactions to give compounds of the general type $[MO_x(OH)_y(OSiR_3)_{z-y-2x}]_n$.[33] This was also observed upon hydrolysis of the bismuth compounds $[Bi(OSiR_2R')_3]$ (R = R′ = Me, Et, *i*Pr; R = Me, R′ = *t*Bu), as indicated by elemental analyses (C, H) and the IR spectra of the dried powders [Eq. (5)].

$$n\,[Bi(OSiR_3)_3] + (l+m)\,H_2O \rightarrow [Bi_nO_l(OH)_m(OSiR_3)_{3n-(2l+m)}] + (2l+m)\,R_3SiOH \quad (5)$$

Thermal decomposition of the hydrolysis products $[Bi_nO_l(OH)_m(OSiR_3)_{3n-(2l+m)}]$ gave α-Bi_2O_3, β-Bi_2O_3, $Bi_{12}SiO_{20}$ or $Bi_4Si_3O_{12}$, depending on the triorganosilanolate ligand, the amount of water and the temperature. Thermal decomposition at 750 °C of $[Bi(OSiEt_3)_3]$ and $[Bi(OSi{\it i}Pr_3)_3]$, which had been treated with a slight excess of water ($l+m = 20n$), gave $Bi_{12}SiO_{20}$ (JCPDS No. 80-0627). Under the same conditions, $[Bi(OSiMe_3)_3]$ gave a mixture of $Bi_{12}SiO_{20}$ and $Bi_4Si_3O_{12}$ (JCPDS No. 76-1726). When the hydrolysis of $[Bi(OSiEt_3)_3]$ was carried out with a larger excess of water and the hydrolysis product was heated in vacuo at 150 °C prior to the thermolysis at 750 °C, α-Bi_2O_3 (JCPDS No. 71-2274) was recovered as the final material. Previously, it was shown that thermal decomposition of the hydrolysis product of $[Bi(OSiMe_2{\it t}Bu)_3]$ at 350 °C gave β-Bi_2O_3 and amorphous SiO_2. At higher temperatures, $Bi_{12}SiO_{20}$ is formed.[38] In contrast to $[Bi(OSiEt_3)_3]$, $[Bi(OSi{\it i}Pr_3)_3]$ and $[Bi(OSiMe_2{\it t}Bu)_3]$, the methyl derivative $[Bi(OSiMe_3)_3]$ readily decomposes with elimination of $Me_3SiOSiMe_3$ at moderate temperatures (ca. 80 °C), both in the solid state and in solution.[35] In the presence of alkali metals, the elimination of hexamethyldisiloxane is observed at even lower temperatures.

Attempts to hydrolyse bismuth silanolates by addition of water or by slow evaporation of the solvent under constant humidity (15, 32 and 45 %) gave amorphous solids. However, exposing the bismuth silanolate solutions to air moisture and crystallising at 4 °C or slowly evaporating the solvent gave single crystals of $[Bi_4O_2(OSiEt_3)_8]$ (**5**), $[Bi_9O_7(OSiMe_3)_{13}]$ (**6**), $[Bi_{18}O_{18}(OSiMe_3)_{18}]$ (**7**), $[Bi_{20}O_{18}(OSiMe_3)_{24}]$ (**8**) and the previously described $[Bi_{22}O_{26}(OSiMe_2{\it t}Bu)_{14}]$ (**9**) (Scheme 3).[38] Hydrolysis may be initiated by either passing

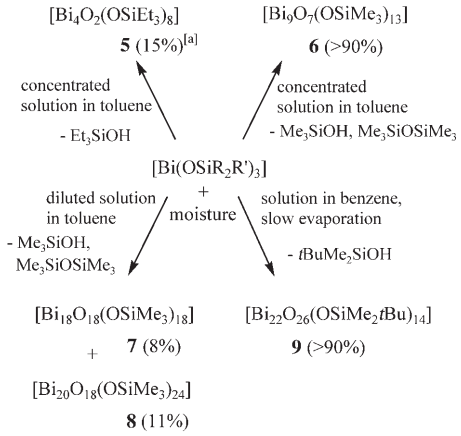

Scheme 3. Crystalline products obtained upon partial hydrolysis of bismuth tris(trialkylsilanolates). Isolated yields are given in brackets. [a] The low isolated yield results from the high solubility of this compound.

a stream of moist air or nitrogen above the solution or by opening the reaction vessel for a short period of time. It is noteworthy that for successful crystallisation of compound **9** the reaction vessel could be fitted with a perforated stopper to allow slow evaporation of the solvent, whereas in the case of compounds **5**–**8** the reaction vessel had to be closed to avoid formation of amorphous solids. The IR spectra of both the crystalline and amorphous solids provide only limited information. However, the IR spectra of the amorphous materials do not correspond to those of the crystalline materials (Figures S1 and S2 in the Supporting Information) and elemental analyses indicate a higher degree of hydrolysis for the amorphous solids (carbon content < 8 %).

The tetranuclear compound **5** (yield 15 %) and the nonanuclear compound **6** (yield > 90 %) were obtained from highly concentrated solutions in toluene, and in the case of the silanolate **5** even from neat liquid $[Bi(OSiEt_3)_3]$. The low isolated yield of compound **5** is a result of its high solubility in all common organic solvents. The high-nuclearity bismuth-oxo clusters **7** and **8** were obtained from dilute solutions in toluene by fractional crystallisation. Notably, after a first batch of single crystals of **8** had been isolated (yield 11 %), a second crop of crystals was obtained. This crystal-

line material was found to be composed of both the octadecanuclear metal-oxo cluster **7** and the eicosanuclear metal-oxo cluster **8**, as shown by single-crystal X-ray diffraction analysis. When this mixture was kept in toluene for several weeks, compound **8** slowly dissolved and compound **7** was exclusively obtained (yield 8%). Apparently, compounds **7** and **8** are in equilibrium and this equilibrium is shifted in favour of **7** either as a result of its low solubility or its higher thermodynamic stability. The ^{29}Si NMR spectrum of the supernatant solution shows a major signal at δ = 7.4 ppm attributable to $Me_3SiOSiMe_3$ and signals of lesser intensity at δ = 6.9, 7.2 and 7.9 ppm. At present, we cannot assign the bismuth-containing species present in solution. NMR studies on the bismuth-oxo clusters are hampered by their poor solubility as well as their moisture sensitivity, and provide little structural information. For example, the ^{1}H NMR spectra of compounds **6** and **8** in [D$_8$]toluene show one single broad signal centred at δ = 0.16 and 0.29 ppm, respectively.

Molecular structures

[Bi$_{18}$Na$_4$(μ$_3$-O)$_4$(μ$_4$-O)$_{15}$(μ$_5$-O)(μ-OSiMe$_3$)$_6$(μ$_3$-OSiMe$_3$)$_{12}$] (2): The heterobimetallic silanolate [Bi$_{18}$Na$_4$O$_{20}$(OSiMe$_3$)$_{18}$] (**2**) crystallises from both pentane and toluene as solvate in the space group $P\bar{1}$ with two formula units per unit cell. Crystallographic data for the toluene solvate are given in Table 1, its molecular structure is shown in Figure 1, and selected bond lengths and bond angles are listed in the figure caption. The molecular structure is composed of 18 bismuth atoms and four sodium atoms, with the metal atoms showing a variety of coordination environments and a broad range of metal–oxygen bond lengths. Two five-coordinated sodium

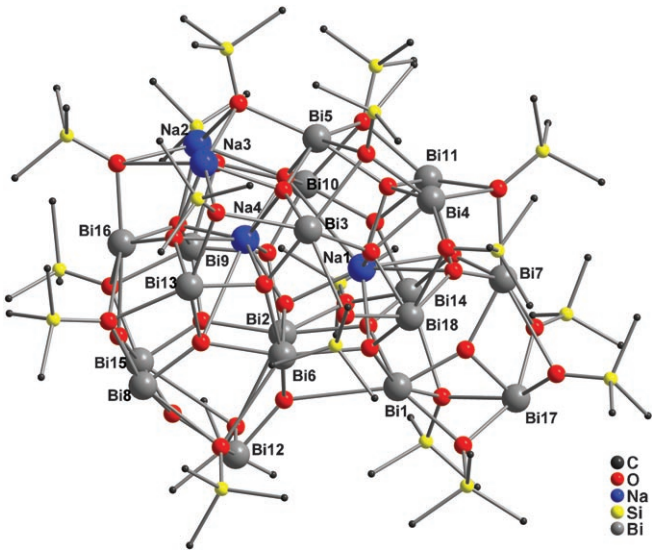

Figure 1. Molecular structure of [Bi$_{18}$Na$_4$(μ$_3$-O)$_4$(μ$_4$-O)$_{15}$(μ$_5$-O)(μ-OSiMe$_3$)$_6$(μ$_3$-OSiMe$_3$)$_{12}$] (**2**). Selected bond lengths [Å] depending on the coordination number (CN) at the bismuth atoms and bond angles [°]: Bi–O (CN = [3+2], Bi9–Bi11, Bi13) 2.048(9)–2.227(8), 2.417(1)–2.563(9); Bi–O (CN = [3+3], Bi3, Bi7, Bi16) 2.089(8)–2.221(9), 2.526(9)–3.198(10); Bi–O (CN = 4, Bi12) 2.049(9)–2.308(8); Bi–O (CN = [4+1], Bi8, Bi14, Bi15) 2.035(8)–2.372(10), 2.759(9)–3.278(10); Bi–O (CN = [4+2], Bi5) 2.063(8)–2.415(8), 2.879(8)–2.947(8); Bi–O (CN = 5, Bi17, Bi18) 2.132(9)–2.495(9); Bi–O (CN = [5+1], Bi1, Bi4, Bi6) 2.127(8)–2.482(10), 2.809(8)–3.185(10); Bi–O (CN = [5+2], Bi2) 2.111(8)–2.437(8), 2.991(9)–3.006(9); Na–O 2.123(10)–3.455(10) (av 2.550); Bi-μ$_3$-O-Bi 100.4(4)–147.2(4) (av 118.3); Bi-μ$_4$-O-Bi 86.3(3)–136.7(4) (av 107.8); Bi-μ$_4$-O-M (M = Na, Bi; 3×Bi, 1×Na) 75.0(3)–141.2(5) (av 106.4); M-μ$_4$-O-M (M = Na, Bi; 2×Bi, 2×Na) 84.5(3)–131.1(4) (av 109.0); *trans*-Na-μ$_5$-O-Na 147.8(4), *cis*-M-μ$_5$-O-M 67.3(3)–131.0(4) (M = Na, Bi).

Table 1. Crystallographic data for [Bi$_{18}$Na$_4$O$_{20}$(OSiMe$_3$)$_{18}$] (**2**), [Bi$_{33}$NaO$_{38}$(OSiMe$_3$)$_{24}$]·3C$_7$H$_8$ (**3**·3C$_7$H$_8$), [Bi$_{50}$Na$_2$O$_{64}$(OH)$_2$(OSiMe$_3$)$_{22}$]·2C$_7$H$_8$·2H$_2$O (**4**·2C$_7$H$_8$·2H$_2$O) and [Bi$_4$O$_2$(OSiEt$_3$)$_8$] (**5**).

	2	**3**·3C$_7$H$_8$	**4**·2C$_7$H$_8$·2H$_2$O	**5**
empirical formula	$C_{54}H_{162}Bi_{18}Na_4O_{38}Si_{18}$	$C_{72}H_{216}Bi_{33}NaO_{62}Si_{24}$·3C$_7H_8$	$C_{66}H_{198}Bi_{50}Na_2O_{88}Si_{22}$·2C$_7H_8$·2H$_2$O	$C_{48}H_{120}Bi_4O_{10}Si_8$
formula weight	5779.06	9944.34	13715.49	1918.08
temperature [K]	173	143	143	173
crystal system	triclinic	monoclinic	monoclinic	monoclinic
space group	$P\bar{1}$	$P2_1/n$	$P2_1/n$	$P2_1/c$
a [Å]	17.0337(9)	20.488(4)	20.0518(12)	25.256(5)
b [Å]	19.5750(14)	22.539(5)	24.1010(15)	15.372(3)
c [Å]	26.6799(16)	26.154(5)	27.4976(14)	21.306(4)
α [°]	72.691(4)			
β [°]	73.113(4)	100.79(3)	103.973(3)	113.96(3)
γ [°]	70.985(4)			
volume [Å^3]	7842.9(8)	11864(4)	12896(1)	7559(3)
Z	2	2	2	4
ρ_{calcd} [g cm^{-3}]	2.447	2.784	3.532	1.685
absorption coefficient [mm^{-1}]	20.309	24.548	34.136	9.453
crystal size [mm]	0.13×0.13×0.03	0.13×0.03×0.03	0.12×0.12×0.02	0.35×0.15×0.10
θ range for data collection [°]	2.92 to 25.37	2.93 to 25.38	2.91 to 25.00	2.94 to 25.07
reflections collected	82794	126243	93902	73572
reflections unique	28558	21400	22595	13347
	[R_{int} = 0.079]	[R_{int} = 0.088]	[R_{int} = 0.085]	[R_{int} = 0.107]
R [$I>2\sigma(I)$]	0.0475	0.0478	0.0761	0.0785
wR_2 (all data)	0.0899	0.0995	0.1652	0.2122
largest diff. peak/hole [e Å^{-3}]	3.209/−1.933	1.443/−1.361	3.850/−2.421	7.434/−1.669

atoms, Na2 and Na3, with Na–O distances in the range 2.32(1)–3.15(1) Å are found at the periphery of the metal-oxo cluster. The sodium atoms Na4 and Na1 show eight- and ninefold coordination, respectively, with Na–O distances in the range 2.12(1)–3.46(1) Å. The sodium atoms do not show any preferred coordination geometry, whereas strongly distorted but distinct coordination polyhedra can be assigned to the bismuth atoms. The distortions may be assigned to the stereochemical activity of the lone pair at the bismuth atoms. The coordination polyhedra are best described as oxygen-capped pseudo-tetrahedra with [3+2]-(Bi9–Bi11, Bi13) and [3+3]-coordination (Bi3, Bi7, Bi16), as regular and oxygen-capped pseudo-trigonal bipyramids with 4- (Bi12), [4+1]- (Bi8, Bi14, Bi15) and [4+2]-coordination (Bi5), and as regular and oxygen-capped pseudo-octahedra with 5- (Bi17, Bi18), [5+1]- (Bi1, Bi4, Bi6) and [5+2]-coordination (Bi2). The Bi–O distances are found in the broad range 2.035(8)–3.28(1) Å, with the primary bonds showing an upper limit of approximately 2.20 Å for pseudo-tetrahedral coordination and approximately 2.50 Å in the case of pseudo-trigonal bipyramidal and pseudo-octahedral coordination. The metal-oxo core of cluster **2** is composed of four μ_3-oxo ligands connected to three bismuth atoms, ten μ_4-oxo ligands connected to three bismuth atoms and a sodium atom, four μ_4-oxo ligands connected to two bismuth and two sodium atoms, one μ_4-oxo ligand connected to four bismuth atoms and one μ_5-oxo ligand connected to two bismuth and three sodium atoms. Most remarkably, coordination of three bismuth atoms to the μ_3-oxo and μ_4-oxo ligands results in a nearly planar trinuclear [Bi_3O] moiety, regardless of the bridging mode of the ligand. A nearly tetrahedral μ_4-oxo ligand is observed if two sodium atoms and two bismuth atoms are involved in the metal–oxygen coordination. The heterometallic oxo core of **2** is embedded in a hydrophobic shell composed of six μ-$OSiMe_3$ and 12 μ_3-$OSiMe_3$ ligands, which show average M–O bond lengths of 2.48 and 2.63 Å, respectively.

[$Bi_4(\mu_3$-$O)_2(\mu$-$OSiEt_3)_6(OSiEt_3)_2$] (5): The bismuth-oxo silanolate [$Bi_4O_2(OSiEt_3)_8$] (**5**) is highly soluble in common organic solvents such as toluene, benzene, CH_2Cl_2, THF and pentane. Single crystals of **5** were obtained from a concentrated solution of [$Bi(OSiEt_3)_3$] in toluene as well as from neat [$Bi(OSiEt_3)_3$]. Compound **5** crystallises in the space group $P2_1/c$ with four formula units in the unit cell. Two crystallographically independent molecules are observed in the crystal lattice, which do not show marked differences in their bond lengths and angles. Thus, only one molecule is discussed in more detail. Crystallographic data are given in Table 1, its molecular structure is shown in Figure 2, and selected bond lengths and angles are listed in the figure caption. The molecular structure of [$Bi_4(\mu_3$-$O)_2(\mu$-$OSiEt_3)_6$-$(OSiEt_3)_2$] (**5**) is best described as being composed of the subunit [$Bi_2(\mu_3$-$O)_2(OSiEt_3)_2$] coordinated by two [$Bi(OSiEt_3)_3$] molecules. This description is consistent with the dynamic behaviour of compound **5** in solution, which is indicated by one set of resonances for the ethyl groups in the

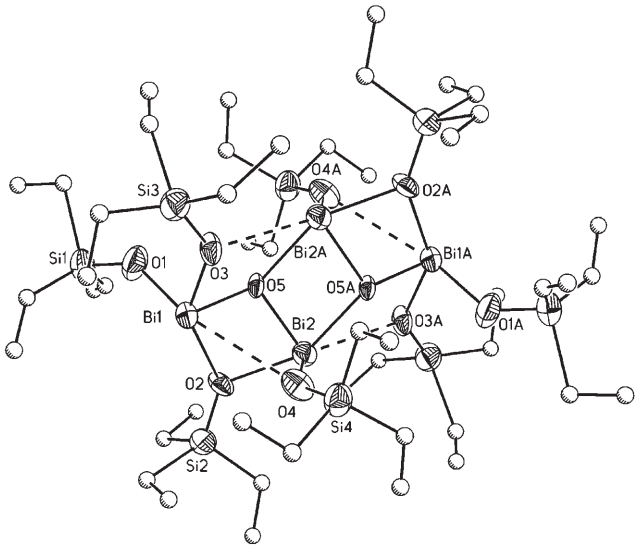

Figure 2. Molecular structure of [$Bi_4(\mu_3$-$O)_2(\mu$-$OSiEt_3)_6(OSiEt_3)_2$] (**5**) showing 30% displacement ellipsoids for bismuth, silicon and oxygen atoms and the atom numbering scheme. The carbon atoms are represented by open circles and hydrogen atoms are omitted for clarity. Only one of the two crystallographically independent molecules present in the unit cell is shown. Selected bond lengths [Å] and bond angles [°]: Bi1–O1 2.07(2), Bi1–O2 2.61(1), Bi1–O3 2.14(1), Bi1–O4 3.10(2), Bi1–O5 2.05(1), Bi2–O2 2.19(1), Bi2–O4 2.10(2), Bi2–O5 2.13(1), Bi2–O3A 3.05(1), Bi2–O5A 2.36(1); O1-Bi1-O2 103.4(6), O1-Bi1-O3 93.6(6), O1-Bi1-O4 154.5(6), O1-Bi1-O5 92.3(6), O2-Bi1-O3 146.1(4), O2-Bi1-O4 59.6(4), O2-Bi1-O5 69.0(4), O3-Bi1-O4 93.4(5), O3-Bi1-O5 81.4(5), O4-Bi1-O5 64.7(4), O2-Bi2-O4 83.9(5), O2-Bi2-O5 76.8(5), O2-Bi2-O3A 144.2(4), O2-Bi2-O5A 149.1(4), O4-Bi2-O5 86.4(6), O4-Bi2-O3A 129.5(5), O4-Bi2-O5A 86.1(5), O5-Bi2-O3A 113.1(4), O5-Bi2-O5A 73.4(4), O3A-Bi2-O5A 59.0(4).

^{1}H NMR spectrum. The bismuth atoms Bi1 and Bi2 in compound **5** are both five-coordinate, but show different coordination polyhedra (Figure 3). An oxygen-capped pseudo-tetrahedron with [3+2]-coordination is assigned to Bi1, with primary Bi–O bonds Bi1–O1 2.07(2), Bi1–O3 2.14(1) and Bi1–O5 2.05(1) Å, and secondary bonds Bi1–O2 2.61(1) and Bi1–O4 3.10(2) Å. An oxygen-capped pseudo-trigonal bipyramid with [4+1]-coordination is assigned to Bi2, with primary Bi–O bonds Bi2–O2 2.19(1), Bi2–O4 2.10(2), Bi2–O5 2.13(1), Bi2–O5A 2.36(1) Å, and a secondary bond Bi2–O3A 3.05(1) Å.

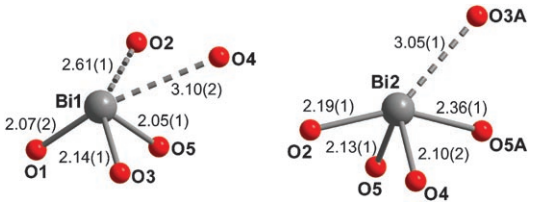

Figure 3. Coordination polyhedra observed for the bismuth atoms in [$Bi_4(\mu_3$-$O)_2(\mu$-$OSiEt_3)_6(OSiEt_3)_2$] (**5**).

$[Bi_9(\mu_3\text{-}O)_4(\mu_4\text{-}O)_3(\mu\text{-}OSiMe_3)_{12}(\mu_3\text{-}OSiMe_3)]$ (6): After exposure of a concentrated solution of $[Bi(OSiMe_3)_3]$ in toluene to air moisture, single crystals of $[Bi_9(\mu_3\text{-}O)_4(\mu_4\text{-}O)_3(\mu\text{-}OSiMe_3)_{12}(\mu_3\text{-}OSiMe_3)]$ (**6**) were obtained at 4 °C. The compound crystallises in the space group $P\bar{1}$ with two formula units in the unit cell. Crystallographic data of compound **6** are given in Table 2, its molecular structure is shown in Figure 4, and selected bond lengths and angles are listed in the figure caption. The molecular structure of the bismuth-oxo silanolate **6** is composed of nine bismuth atoms showing a variety of BiO_n coordination polyhedra (see below), and four μ_3-oxo and three μ_4-oxo ligands. One μ_3-$OSiMe_3$ and 12 μ-$OSiMe_3$ ligands are found at the periphery of the metal-oxo cluster. The stereochemical activity of the lone pair at the bismuth atoms is indicated by the strongly distorted coordination polyhedra, which are best described as oxygen-capped pseudo-tetrahedra with [3+2]-coordination for Bi7, Bi8 and Bi9, as oxygen-capped pseudo-trigonal bipyramids with [4+1]-coordination for Bi4, [4+2]-coordination for Bi1 and Bi2 and as oxygen-capped pseudo-octahedra with [5+1]-coordination for Bi3, Bi5 and Bi6. The Bi–O distances are found to be in the range 2.08–3.00 Å, with the primary bonds showing an upper limit of approximately 2.20 Å for [3+2]-coordination and 2.60 Å for [4+1]- and [5+1]-coordination. However, it is difficult to distinguish between [3+2]-coordination and distorted pseudo-trigonal bipyramidal coordination. Formally, the metal-oxo cluster **6** can be divided into a cationic $[Bi_6O_8]^{2+}$ fragment (**A**), an Me_3Si cation and three anionic $[Bi(OSiMe_3)_4]^-$ units coordinated to the central metal-oxo core **A** (Figure 5). The hexanuclear unit **A** is the most common structural motif reported for bismuth-oxo compounds and is realised in bismuth-oxo(hydroxy) nitrates,[41] bismuth-oxo(hydroxy) perchlorates,[42] bismuth-oxo alkoxides,[23,31,32] and bismuth-oxo carboxylates.[43,44]

Table 2. Crystallographic data for $[Bi_9O_7(OSiMe_3)_{13}]\cdot 0.5\,C_7H_8$ (**6**·0.5 C_7H_8), $[Bi_{18}O_{18}(OSiMe_3)_{18}]\cdot 2\,C_7H_8$ (**7**·2 C_7H_8) and $[Bi_{20}O_{18}(OSiMe_3)_{24}]\cdot 3\,C_7H_8$ (**8**·3 C_7H_8).

	6·0.5 C_7H_8	**7**·2 C_7H_8	**8**·3 C_7H_8
empirical formula	$C_{39}H_{117}Bi_9O_{20}Si_{13}\cdot 0.5\,C_7H_8$	$C_{54}H_{162}Bi_{18}O_{36}Si_{18}\cdot 2\,C_7H_8$	$C_{72}H_{216}Bi_{20}O_{42}Si_{24}\cdot 3\,C_7H_8$
formula weight	3198.38	5839.36	6884.61
temperature [K]	143	143	173
crystal system	triclinic	triclinic	triclinic
space group	$P\bar{1}$	$P\bar{1}$	$P\bar{1}$
a [Å]	15.1916(9)	14.8295(12)	17.2915(14)
b [Å]	15.2439(13)	16.1523(13)	18.383(2)
c [Å]	22.487(5)	18.4166(17)	18.4014(18)
α [°]	79.686(3)	75.960(4)	95.120(5)
β [°]	74.540(5)	79.112(4)	115.995(5)
γ [°]	66.020(4)	63.789(4)	106.813(5)
volume [Å^3]	4571(1)	3822.5(6)	4171.6(8)
Z	2	1	1
ρ_{calcd} [g cm^{-3}]	2.324	2.537	2.347
absorption coefficient [mm^{-1}]	17.477	20.825	18.187
crystal size [mm]	0.25 × 0.10 × 0.04	0.18 × 0.13 × 0.05	0.08 × 0.05 × 0.03
θ range for data collection [°]	2.93 to 27.50	2.91 to 27.48	2.92 to 27.50
reflections collected	87444	51518	79183
reflections unique	20928	17451	22203
	[R_{int} = 0.119]	[R_{int} = 0.049]	[R_{int} = 0.056]
R [$I > 2\sigma(I)$]	0.0385	0.0359	0.0341
wR_2 (all data)	0.0711	0.0666	0.0619
largest diff. peak/hole [e Å^{-3}]	2.002/−2.455	1.506/−1.429	1.718/−1.214

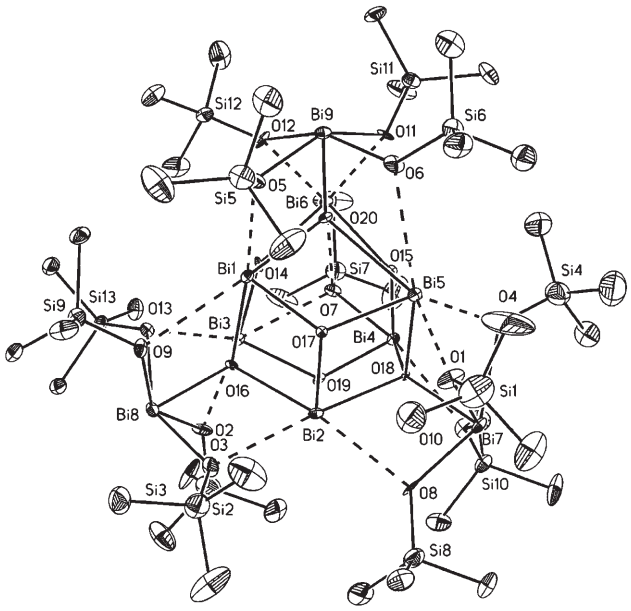

Figure 4. Molecular structure of $[Bi_9(\mu_3\text{-}O)_4(\mu_4\text{-}O)_3(\mu\text{-}OSiMe_3)_{12}(\mu_3\text{-}OSiMe_3)]$ (**6**) showing 30% displacement ellipsoids and the atom numbering scheme. Hydrogen atoms are omitted for clarity. Selected bond lengths [Å] depending on the coordination number (CN) at the bismuth atom and bond angles [°]: Bi–O (CN = [3+2], Bi7–Bi9) 2.082(6)–2.196(6), 2.329(6)–2.583(7); Bi–O (CN = [4+1], Bi4) 2.088(6)–2.373(7), 2.789(8); Bi–O (CN = [4+2], Bi1, Bi2) 2.137(6)–2.392(6), 2.751(6)–2.950(7); Bi–O (CN = [5+1], Bi3, Bi5, Bi6) 2.151(6)–2.374(6), 2.717(6)–2.999(7); Bi-μ-$OSiMe_3$-Bi 88.6(2)–99.2(2) (av 95.1); Bi-μ_3-$OSiMe_3$-Bi 86.9(2), 92.6(2), 94.9(2) (av 91.5); Bi-μ_3-O-Bi 106.7(3)–131.7(3) (av 115.6); Bi-μ_4-O-Bi 100.1(2)–123.0(3) (av 109.2).

$[Bi_{18}(\mu_3\text{-}O)_{12}(\mu_4\text{-}O)_6(\mu\text{-}OSiMe_3)_{10}(\mu_3\text{-}OSiMe_3)_6(OSiMe_3)_2]$ (7) and $[Bi_{20}(\mu_3\text{-}O)_{10}(\mu_4\text{-}O)_8(\mu\text{-}OSiMe_3)_{16}(\mu_3\text{-}OSiMe_3)_4(OSiMe_3)_4]$ (8): Single crystals of $[Bi_{18}(\mu_3\text{-}O)_{12}(\mu_4\text{-}O)_6(\mu\text{-}OSiMe_3)_{10}(\mu_3\text{-}OSiMe_3)_6(OSiMe_3)_2]$ (**7**) and $[Bi_{20}(\mu_3\text{-}O)_{10}(\mu_4\text{-}O)_8(\mu\text{-}OSiMe_3)_{16}(\mu_3\text{-}OSiMe_3)_4(OSiMe_3)_4]$ (**8**) were obtained as toluene solvates from a dilute solution of $[Bi(OSiMe_3)_3]$ in toluene at 4 °C that had been exposed to air moisture. Compounds **7** and **8** both crystallise in the space group $P\bar{1}$ with one formula unit per unit cell. Crystallographic data of compounds **7** and **8** are given in Table 2, the molecular structures are shown in Figures 6 and 7, and selected bond lengths and angles are listed in the figure captions.

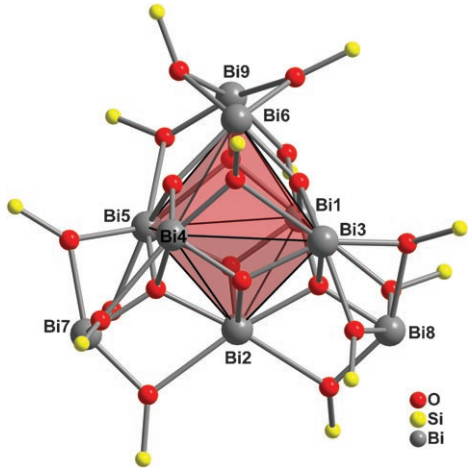

Figure 5. View of the central hexanuclear motif $[Bi_6O_8]^{2+}$ (**A**) (oxygen-capped red octahedron) in $[Bi_9(\mu_3\text{-}O)_4(\mu_4\text{-}O)_3(\mu\text{-}OSiMe_3)_{12}(\mu_3\text{-}OSiMe_3)]$ (**6**). Carbon atoms are omitted for clarity.

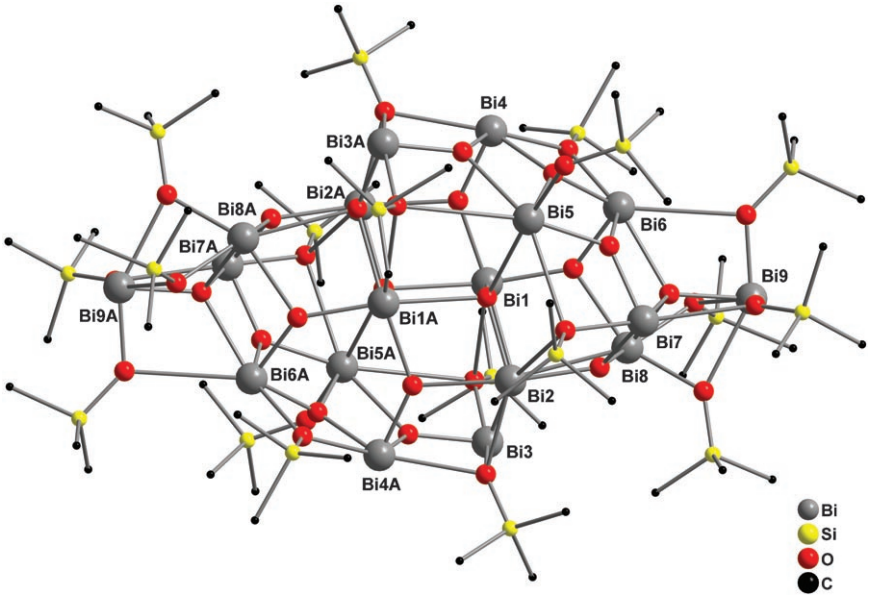

Figure 6. Molecular structure of $[Bi_{18}(\mu_3\text{-}O)_{12}(\mu_4\text{-}O)_6(\mu\text{-}OSiMe_3)_{10}(\mu_3\text{-}OSiMe_3)_6(OSiMe_3)_2]$ (**7**). Selected bond lengths [Å] depending on the coordination number (CN) at the bismuth atoms and bond angles [°]: Bi–O (CN = [3+1], Bi3) 2.028(6)–2.127(7), 2.501(6); Bi–O (CN = [3+2], Bi4, Bi9) 2.050(5)–2.193(6), 2.415(6)–2.683(6); Bi–O (CN = [3+3], Bi1, Bi2, Bi5) 2.077(6)–2.273(5), 2.433(5)–3.324(6); Bi–O (CN = [4+1], Bi7) 2.071(6)–2.330(5), 2.864(6); Bi–O (CN = [5+1], Bi6, Bi8) 2.0915–2.496(6), 2.944(6)–3.172(6); Bi-μ-$OSiMe_3$-Bi 88.8(2)–101.8(2) (av 95.3); Bi-μ_3-$OSiMe_3$-Bi 78.1(2)–93.8(2) (av 90.6); Bi-μ_3-O-Bi 102.6(2)–135.2(3) (av 117.5); Bi-μ_4-O-Bi 90.0(2)–125.1(2) (av 108.8).

The molecular structure of the metal-oxo cluster **7** is composed of 18 bismuth atoms, 12 μ_3-oxo and six μ_4-oxo ligands within the metal-oxo core, and ten μ-$OSiMe_3$, six μ_3-$OSiMe_3$ and two terminal $OSiMe_3$ ligands at the periphery of the metal-oxo cluster. Strongly distorted coordination polyhedra at the bismuth atoms are observed. Oxygen-capped pseudo-tetrahedra with [3+1]-coordination are assigned to Bi3, with [3+2]-coordination to Bi4 and Bi9, and with [3+3]-coordination to Bi1, Bi2 and Bi5. The primary Bi–O bonds are observed in the range 2.028(6)–2.273(5) Å and the secondary bonds are in the range 2.415(6)–3.324(6) Å. The coordination at Bi7 is best described as oxygen-capped pseudo-trigonal-bipyramidal with bond lengths of 2.071(6)–2.330(5) Å and 2.864(6) Å. Oxygen-capped pseudo-octahedra with [5+1]-coordination are observed for Bi6 and Bi8.

The molecular structure of compound **8** comprises 20 bismuth atoms, ten μ_3-oxo and eight μ_4-oxo ligands within the metal-oxo core, and 16 μ-$OSiMe_3$, four μ_3-$OSiMe_3$ and four terminal $OSiMe_3$ ligands at the periphery. The following bismuth–oxygen coordination polyhedra are found: monocapped pseudo-tetrahedra for Bi1, Bi4, Bi9 and Bi10, bicapped pseudo-tetrahedra for Bi2 and Bi3, a monocapped pseudo-trigonal bipyramid for Bi7, and monocapped pseudo-octahedra for Bi6 and Bi8. The bismuth–oxygen distances are in the same range as those observed for the metal-oxo cluster **7**.

The most striking common feature of the two bismuth-oxo clusters **7** and **8** is the substructure $[Bi_{16}O_{18}(OSiMe_3)_{12}]$ (**B**), which is based on four edge-sharing octahedral $\{Bi_6\}$ units of type **A** (Figure 8). In unit **B**, the trigonal faces of the $\{Bi_6\}$ units are capped by oxo and $OSiMe_3$ ligands. Two $OSiMe_3$ ligands in compound **8** were formally assigned as terminal ligands, but show weak Bi–O interactions with bond lengths of 3.739 and 3.685 Å to bismuth atoms placed on a trigonal face of a $\{Bi_6\}$ unit. The molecular structures of the bismuth-oxo clusters **7** and **8** can be derived from $[Bi_{16}O_{18}(OSiMe_3)_{12}]$ (**B**) by adding two and four $[Bi(OSiMe_3)_3]$ molecules, respectively. Slightly different structural arrangements of the oxo and $OSiMe_3$ ligands are observed for compounds **7** and **8**, but with only minor perturbation of the $\{Bi_6\}$ units **A** (Figure 8). The bismuth silanolate fragments at the periphery of the bismuth-oxo clusters might be formulated as $[Bi(OSiMe_3)_4]^-$ anions, which are coordinated to an oxo ligand of unit **B**. The geometry at these bismuth atoms (**7**, Bi9; **8**, Bi9, Bi10) is best described as [3+2]-coordination. In both compounds, the bismuth atom Bi9 exhibits a short Bi–O distance to the oxo ligand of unit **B** (**7**, Bi9–O9 2.113(5) Å; **8**, Bi9–O16 2.090(5) Å). In contrast, the Bi–O distance of Bi10 to the oxo ligand of the central metal-oxo core in compound **8** is larger and amounts to 2.638(5) Å (Figure 7). Furthermore, Bi9 in compounds **7** and **8** is linked to unit **B** by four μ-$OSiMe_3$ ligands, whereas Bi10 is coordinated to three μ-$OSiMe_3$ ligands. Thus, in com-

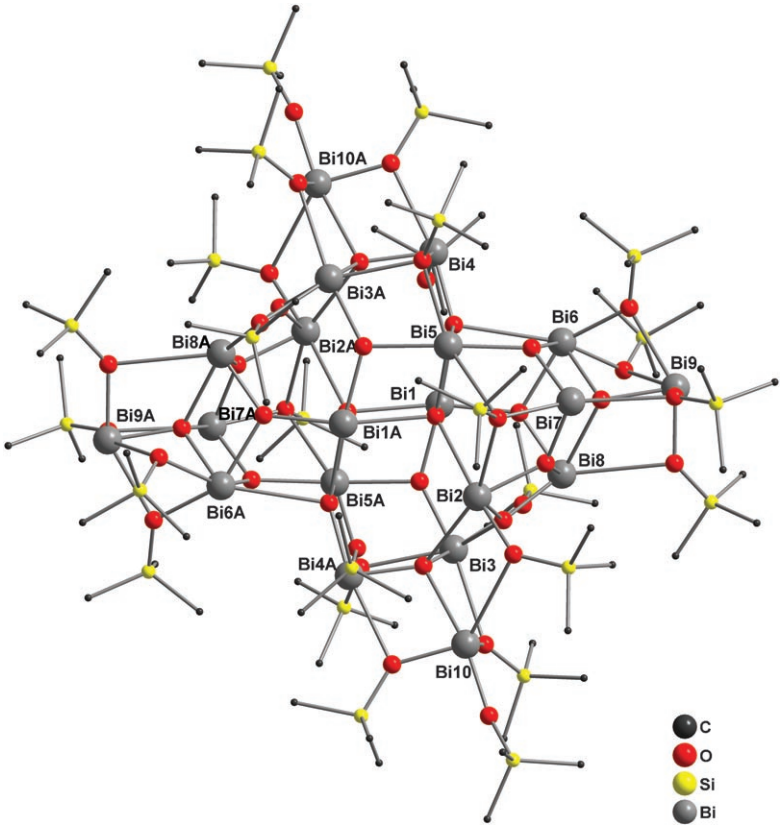

Figure 7. Molecular structure of $[Bi_{20}(\mu_3\text{-}O)_{10}(\mu_4\text{-}O)_8(\mu\text{-}OSiMe_3)_{16}(\mu_3\text{-}OSiMe_3)_4(OSiMe_3)_4]$ (**8**). Selected bond lengths [Å] depending on the coordination number (CN) at the bismuth atoms and bond angles [°]: Bi–O (CN = [3+2], Bi1, Bi4, Bi9, Bi10) 2.067(5)–2.209(5), 2.448(5)–3.125(6); Bi–O (CN = [3+3], Bi2, Bi3) 2.085(5)–2.211(6), 2.528(5)–2.900(6); Bi–O (CN = [4+1], Bi7) 2.083(5)–2.300(6), 2.881(6); Bi–O (CN = [5+1], Bi5, Bi6, Bi8) 2.081(5)–2.569(5), 2.968(6)–3.137(6); Bi-μ-OSiMe$_3$-Bi 89.3(2)–102.9(2) (av 97.5); Bi-μ_3-OSiMe$_3$-Bi 90.0(2)–95.6(2) (av 93.1); Bi-μ_3-O-Bi 105.8(2)–131.0(3) (av 117.6); Bi-μ_4-O-Bi 88.2(2)–133.3(3) (av 108.8).

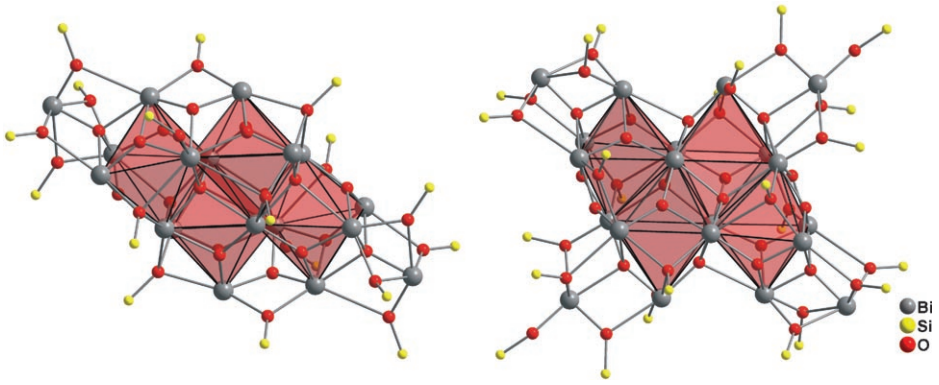

Figure 8. Views of the metal-oxo frameworks of $[Bi_{18}(\mu_3\text{-}O)_{12}(\mu_4\text{-}O)_6(\mu\text{-}OSiMe_3)_{10}(\mu_3\text{-}OSiMe_3)_6(OSiMe_3)_2]$ (**7**, left) and $[Bi_{20}(\mu_3\text{-}O)_{10}(\mu_4\text{-}O)_8(\mu\text{-}OSiMe_3)_{16}(\mu_3\text{-}OSiMe_3)_4(OSiMe_3)_4]$ (**8**, right). The octahedral $\{Bi_6\}$ units **A** which constitute the substructure $[Bi_{16}O_{18}(OSiMe_3)_{12}]$ (**B**) are highlighted in red. Carbon atoms are omitted.

pound **8** dissociation of $[Bi(OSiMe_3)_3]$ in solution is most likely to occur first at the site of Bi10 coordination. The structural features discussed here support the hypothesis that compounds **7** and **8** are in equilibrium (see results), probably together with $[Bi(OSiMe_3)_3]$. This aspect will be addressed in more detail in future work.

$[Bi_{33}Na(\mu_3\text{-}O)_{10}(\mu_4\text{-}O)_{26}(\mu_6\text{-}O)_2(\mu\text{-}OSiMe_3)_{12}(\mu_3\text{-}OSiMe_3)_{12}]$ (3): The heterobimetallic silanolate $[Bi_{32}(Bi_{0.5}/Na_{0.5})_2(\mu_3\text{-}O)_{10}(\mu_4\text{-}O)_{26}(\mu_6\text{-}O)_2(\mu\text{-}OSiMe_3)_{12}(\mu_3\text{-}OSiMe_3)_{12}]$ (**3**) crystallises from toluene in the space group $P2_1/n$ with two formula units per unit cell. Crystallographic data are given in Table 1, its molecular structure is shown in Figure 9, and selected bond lengths and angles are listed in the figure caption. The molecular structure of the heterobimetallic compound **3** is composed of 33 bismuth atoms and one sodium atom. The sodium atom and one bismuth atom (M17, M = Bi, Na) are disordered and occupy the same position with an occupancy of 50% for each metal. In total, 17 crystallographically independent positions are observed for the metal atoms as a result of a centre of inversion. The metal-oxo core of compound **3** is composed of 38 oxo and 24 $OSiMe_3$ ligands. The latter are placed at the periphery of the cluster and half of the $OSiMe_3$ ligands are μ- and the other half μ_3-bridging. In addition to the ten μ_3-oxo and 26 μ_4-oxo ligands, two μ_6-oxo ligands are observed. The existence of μ_6-oxo ligands is attributed to the presence of sodium atoms and has been reported previously for heterobimetallic sodium–bismuth-oxo clusters.[26,40,45]

As has been noted for other bismuth-oxo clusters, a variety of coordination geometries for the bismuth atoms are observed in compound **3**, including coordination numbers of [3+1], [3+2], [3+3], [4+1], [4+2], [4+3], 5, [5+2], [6+2] and 9. This demonstrates the variable and rich coordination chemistry of the bismuth atom, which often makes structure prediction for bismuth-

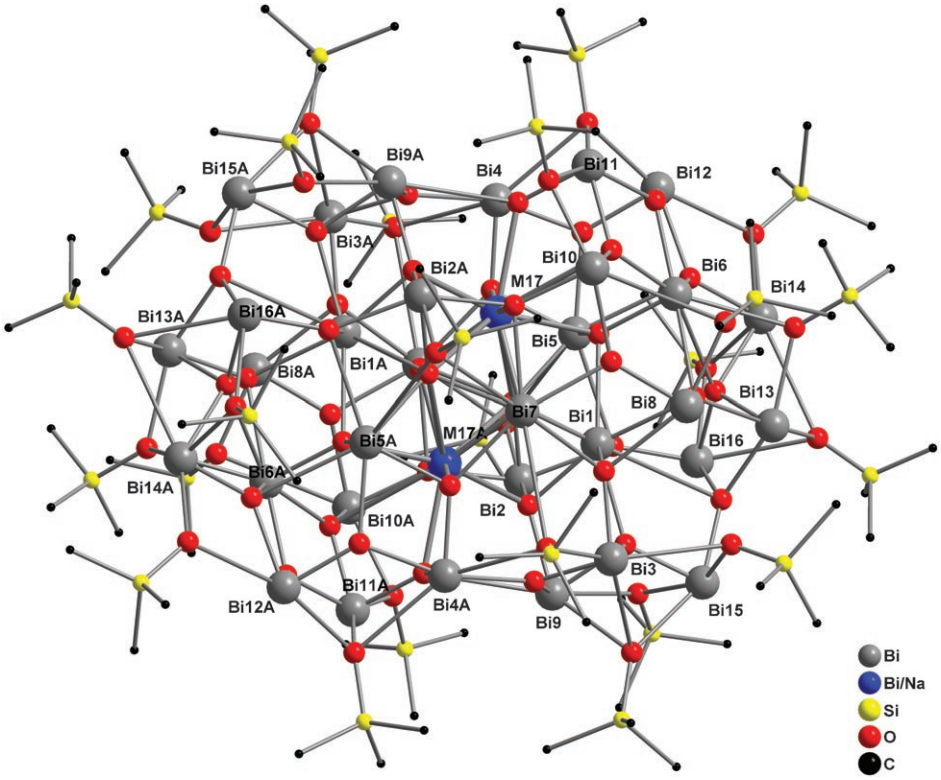

Figure 9. Molecular structure of $[Bi_{32}(Bi_{0.5}/Na_{0.5})_2(\mu_3\text{-}O)_{10}(\mu_4\text{-}O)_{26}(\mu_6\text{-}O)_2(\mu\text{-}OSiMe_3)_{12}(\mu_3\text{-}OSiMe_3)_{12}]$ (**3**). Selected bond lengths [Å] depending on the coordination number (CN) at the bismuth atoms and bond angles [°]: Bi–O (CN = [3+1], Bi8) 2.03(1)–2.17(1), 2.52(1); Bi–O (CN = [3+2], Bi11, Bi16) 2.02(1)–2.19(1), 2.52(1)–2.93(1); Bi–O (CN = [3+3], Bi9) 2.12(1)–2.160(9), 2.48(1)–3.19(1); Bi–O (CN = [4+1], Bi10, Bi12) 2.04(1)–2.40(1), 2.97(1)–3.19(1); Bi–O (CN = [4+2], Bi3, Bi4, Bi14) 2.06(1)–2.445(9), 2.97(1)–3.06(1); Bi–O (CN = [4+3], Bi5) 2.10(1)–2.37(1), 2.75(1)–3.32(1); Bi–O (CN = 5, Bi2, Bi13, Bi15) 2.07(1)–2.49(1); Bi–O (CN = [5+2], Bi6) 2.13(1)–2.62(1), 2.94(1)–3.04(1); Bi–O (CN = [6+2], Bi7) 2.08(1)–2.48(1), 3.30(1)–3.43(1); M–O (CN = 7, Bi/Na17) 2.37(1)–2.66(1); Bi–O (CN = 9, Bi1) 2.22(1)–3.38(1); Bi-μ-$OSiMe_3$-Bi 87.8(4)–100.0(5) (av 93.0); Bi-μ_3-$OSiMe_3$-Bi 68.0(4)–99.0(5) (av 85.0); Bi-μ_3-O-Bi 103.1(4)–131.2(5) (av 117.9); Bi-μ_4-O-Bi 85.6(4)–151.0(5) (av 108.7); M-μ_4-O-M (M = Na, Bi) 84.9(4)–137.7(5) (av 108.1).

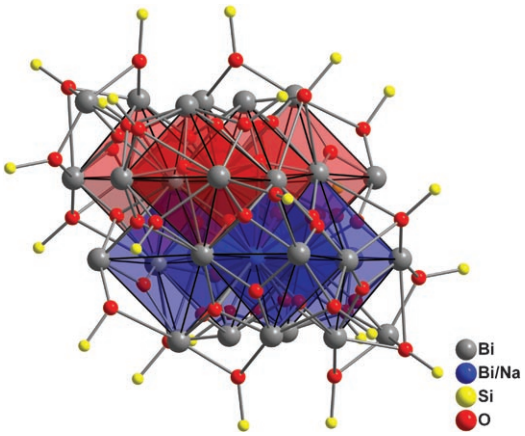

Figure 10. View of the basic structural motif in $[Bi_{32}(Bi_{0.5}/Na_{0.5})_2(\mu_3\text{-}O)_{10}(\mu_4\text{-}O)_{26}(\mu_6\text{-}O)_2(\mu\text{-}OSiMe_3)_{12}(\mu_3\text{-}OSiMe_3)_{12}]$ (**3**). The octahedral $\{Bi_6\}$ units **A** are highlighted in red and in blue. Carbon atoms are omitted.

containing complexes a difficult task. Most remarkably, the metal-oxo cluster **3** is composed of ten edge-sharing $\{Bi_6\}$ units of type **A** (with partial substitution by Na atoms). Two sets of five $\{Bi_6\}$ units can be distinguished, which define two layers. In Figure 10, one set is highlighted in blue and the other in red. The $\{Bi_6\}$ units (**A**) are connected through the edges of the octahedra.

The disordered sodium atom is found in two symmetry-equivalent positions, which are shared by six $\{Bi_6\}$ units. Clearly, the partial exchange of bismuth by sodium atoms does not significantly influence the basic structural motif based on edge-sharing $\{Bi_6\}$ units (**A**), but results in changes in the oxygen sublattice. In compounds **6**–**8**, the octahedral voids of the $\{Bi_6\}$ units (**A**) are not occupied by oxygen atoms, whereas in compound **3** a total of four $\{Bi_6\}$ units (**A**) show inclusion of oxygen atoms (Figure 10). Notably, $[Bi_2Na_4O(OSiMe_3)_8]$ (**1**) is also based on an octahedral $\{M_6\}$ unit (M = Bi, Na), with an oxygen atom occupying the octahedral void inside the metal-oxo cluster.[40]

$[Bi_{50}Na_2(\mu_3\text{-}O)_{18}(\mu_4\text{-}O)_{46}(\mu_3\text{-}OH)_2(\mu_3\text{-}OSiMe_3)_4(\mu\text{-}OSiMe_3)_{18}]$ (4): The heterobimetallic silanolate $[Bi_{50}Na_2O_{64}(OH)_2(OSiMe_3)_{22}]$ (**4**) crystallises from toluene in the space group $P2_1/n$ with two formula units per unit cell. Crystallographic data are given in Table 1, its molecular structure is shown in Figure 11, and selected bond lengths and angles are listed in the figure caption. Compound **4** is obtained as a minor product accompanying the formation of $[Bi_2Na_4O(OSiMe_3)_8]$ (**1**). Its identity was unambiguously established by single-crystal X-ray diffraction analyses of five crystals. The molecular structure of the heterobimetallic silanolate **4** is composed of two sodium atoms and 50 bismuth atoms showing a variety of coordination geometries. The predominant coordination is based on the pseudo-tetrahedron, with Bi–O distances in the range 1.9–2.5 Å. These primary bonds are accompanied by a maximum of six secondary bonds with distances in the range 2.7–3.4 Å. Notably, six bismuth atoms show a coordination geometry that is best described as pseudo-pentagonal-bipyramidal (Bi–O 2.05(2)–2.77(2) Å). This coordination polyhedron was not noticed in any of the other bismuth-oxo clusters. The oxygen sublattice is composed of 18 μ_3- and 46 μ_4-oxo ligands. In addition, two μ_3-OH ligands are located at

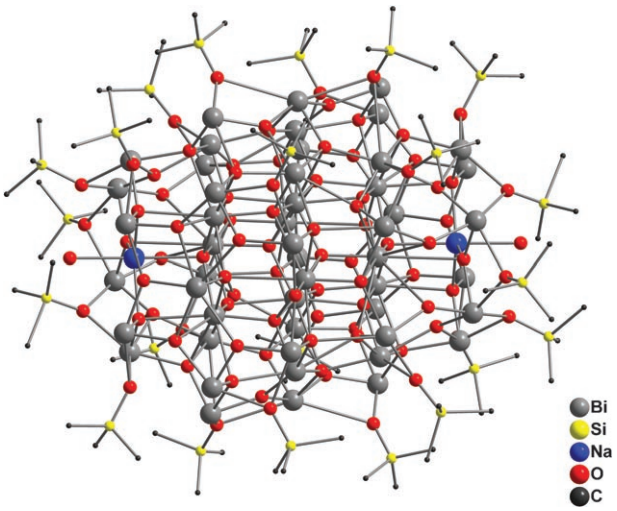

Figure 11. Molecular structure of $[Bi_{50}Na_2(\mu_3\text{-}O)_{18}(\mu_4\text{-}O)_{46}(\mu_3\text{-}OH)_2(\mu_3\text{-}OSiMe_3)_4(\mu\text{-}OSiMe_3)_{18}]$ (**4**). Selected bond lengths [Å] depending on the coordination number (CN) at the bismuth atoms and bond angles [°]; *n* defines the number of bismuth atoms assigned to a coordination number: Bi–O (CN = [3+2], *n* = 1) 2.02(2)–2.27(2), 2.48(2)–2.56(2); Bi–O (CN = 4, *n* = 8) 1.99(2)–2.47(2); Bi–O (CN = [4+1], *n* = 5) 1.97(2)–2.40(2), 2.69(2)–2.84(2); Bi–O (CN = [4+2], *n* = 1) 2.07(2)–2.31(2), 2.99(2)–3.21(2); Bi–O (CN = 6, *n* = 3) 2.05(2)–2.77(2); Bi–O (CN = 7–10, *n* = 7) 2.06(2)–3.41(2); Na–O (CN = 5) 2.23(2)–2.57(2); Bi-μ-$OSiMe_3$-Bi 86.9(8)–97.8(8) (av 92.5); Bi-μ_3-$OSiMe_3$-Bi 73.5(7)–94.4(8) (av 85.9); Bi-μ_3-O-Bi 91.9(8)–150.4(9) (av 117.3); Bi-μ_4-O-Bi 85.8(7)–138.6(9) (av 108.2); M-μ_4-O-M (M = Na, Bi) 81.1(4)–122.2(5) (av 108.0).

the periphery of the bismuth-oxo cluster. A short O(38)–O(42) bond length of 2.49(2) Å is indicative of strong hydrogen bonding between the hydroxy group and a silanolate ligand. The moisture sensitivity of the compound might be explained by the insufficient shielding of the cluster by a total of only 22 $OSiMe_3$ ligands. The metal-oxo core of compound **4** is composed of 20 edge-sharing $\{Bi_6\}$ units of type **A**, which are highlighted in red and blue in Figure 12. Most

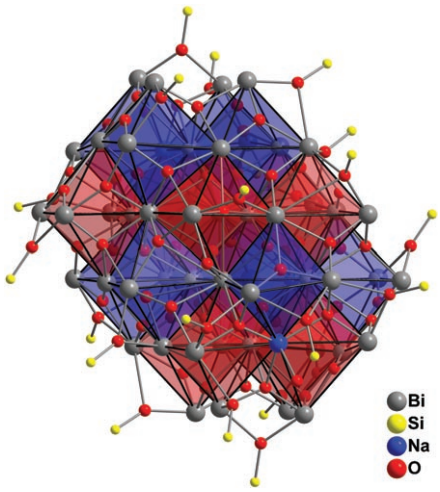

Figure 12. View of the basic metal-oxo core of $[Bi_{50}Na_2O_{64}(OH)_2(OSiMe_3)_{22}]$ (**4**). The octahedral $\{Bi_6\}$ units are highlighted in red and in blue. Carbon atoms are omitted.

of the octahedral voids are empty, with exceptions occurring mainly at the periphery of the metal-oxo cluster. Some of the oxo ligands, which would be expected to be placed on the trigonal faces of the $\{Bi_6\}$ units (**A**), are shifted slightly towards the centre of the octahedron.

Discussion

We have analysed the molecular structures of eight novel homo- and heterometallic bismuth-oxo silanolates, which provide information on the growth process of bismuth-oxo clusters. The molecular structures of the bismuth-rich heterometallic compounds **3** and **4** are closely related to those obtained for the bismuth-oxo clusters **5**–**9**. In contrast, the sodium-rich compound $[Bi_{18}Na_4O_{20}(OSiMe_3)_{18}]$ (**2**), as well as the recently reported sodium–bismuth-oxo silanolates $[Bi_{10}Na_5O_7(OH)_6(OSiMe_3)_{15}]$ and $[Bi_{15}Na_3O_{18}(OSiMe_3)_{12}]$,[40] show only a limited structural relationship with compounds **5**–**9**. This might be attributed to the preferred formation of $[Bi_3(\mu_3\text{-}O)]$ units in bismuth-rich metal-oxo clusters, which is essential for the formation of $\{Bi_6\}$ moieties of type **A** (see below). Substitution of bismuth atoms by sodium atoms partially disrupts this preferred coordination motif as a result of the nondirected coordination bonds to sodium.

The synthesis of homoleptic bismuth silanolates of the general type $[Bi(OSiR_3)_3]$ by a metathesis reaction starting from $BiCl_3$ and $NaOSiR_3$ has been reported for bulky organic groups R such as O*t*Bu.[37] It has been shown that heterobimetallic sodium–bismuth-oxo clusters and $Me_3SiOSiMe_3$ are obtained with $NaOSiMe_3$. In contrast, $[Bi(OtBu)_3]$ is accessible by metathesis reaction.[28]

Homoleptic bismuth silanolates are extremely moisture-sensitive and tend to hydrolyse more rapidly than bismuth alkoxides. Additionally, elimination of siloxanes to give Bi–O–Bi moieties is much easier than ether elimination from metal alkoxides. Another important difference is the fact that the hydrolysis products of the alkoxides are poorly soluble, whereas bismuth-oxo silanolates tend to give large aggregates of the type $[BiO_x(OSiR_3)_{3-y}]_n$ with better solubility properties.

The molecular structures of compounds **5**–**8** are best described as aggregates composed of metal-oxo clusters $[BiO_x(OSiR_3)_{3-y}]_n$ and bismuth silanolate molecules $[Bi(OSiR_3)_3]$. Thus, the bismuth-oxo clusters $[Bi_4O_2(OSiEt_3)_8]$ (**5**), $[Bi_9O_7(OSiMe_3)_{13}]$ (**6**), $[Bi_{18}O_{18}(OSiMe_3)_{18}]$ (**7**) and $[Bi_{20}O_{18}(OSiMe_3)_{24}]$ (**8**) might be described as $[Bi_2O_2(OSiEt_3)_2]\cdot 2[Bi(OSiEt_3)_3]$ (**5**), $[Bi_6O_7(OSiMe_3)_4]\cdot 3[Bi(OSiMe_3)_3]$ (**6**), $[Bi_{16}O_{18}(OSiMe_3)_{12}]\cdot 2[Bi(OSiMe_3)_3]$ (**7**) and $[Bi_{16}O_{18}(OSiMe_3)_{12}]\cdot 4[Bi(OSiMe_3)_3]$ (**8**), respectively. Apparently, the bismuth silanolate coordinates at the periphery of the central metal-oxo cluster to give the final crystalline material.

The first hydrolysis step of $[Bi(OSiR_3)_3]$ is expected to give $[Bi(OH)(OSiR_3)_2]$, and this is followed by condensation to give $[Bi_2O(OSiR_3)_4]_n$. To the best of our knowledge, silanolates and alkoxides of bismuth compounds of this type

have not been reported previously, although related diorganobismuth(III) oxides are known.[46] A primary hydrolysis product, $[Bi_3(OH)(OOCCF_3)_8]$, was recently observed upon partial hydrolysis of bismuth trifluoroacetate, and might be formulated as the coordination compound $[Bi(OH)(OOCCF_3)_2]\cdot 2[Bi(OOCF_3)_3]$.[44] The second hydrolysis/condensation step is expected to give compounds of the type $[BiO(OSiR_3)]_n$. This structure is realised in $[Bi_4O_2(OSiEt_3)_8]$ (**5**) as well as in $[Bi_4O_2(OtBu)_8]$,[47] $[Bi_4O_2(OOCCF_3)_8]$,[48] and in the complex anion $[Bi_2O_2(OH)_6]^{4-}$ found in $Na_6[Bi_2O_2(OH)_6](OH)_2\cdot 2H_2O$.[49] These compounds might be assigned the general formulae $[BiOX]_2\cdot 2BiX_3$ (X = OR, $OSiR_3$, OOCR) and $[BiOX]_2\cdot 4X$ ($X = OH^-$), respectively. It is noteworthy that the hydrolysis of $BiCl_3$ by addition of water results in the formation of BiOCl. This is in agreement with the observation that the bismuth/oxo ligand ratio in the central bismuth-oxo clusters of compounds **5**–**8** is close to one-to-one.

A basic structural motif in the silanolate **5** is the four-membered $[Bi_2O_2]$ ring, which is observed in a variety of bismuth compounds.[23,29,49,50] The $\{Bi_6\}$ unit $[Bi_6O_8]^{2+}$ (**A**) may be described as a closed 3,4-connected net comprising 12 $[Bi_2O_2]$ units. Alternatively, the substructure **A** might be described as an octahedron with the bismuth atoms placed at the corners and the oxygen atoms placed on the trigonal faces. Thus, eight edge-sharing $[Bi_3(\mu_3\text{-}O)]$ units are formed. Such an oxo-centred trinuclear $[Bi_3(\mu_3\text{-}O)]$ unit has been observed in $[Bi_3(OH)(OOCCF_3)_8]$, which is the only example of which we are aware.[44] In contrast, the hexanuclear $\{Bi_6\}$ unit **A** is part of a wide variety of molecular bismuth-oxo clusters.[23,31,32,41–44] It has been suggested that in aqueous solution hexanuclear cations of the type $[Bi_6O_{4+x}(OH)_{4-x}]^{(6-x)+}$ are predominantly found at $pH < 3$ at low concentrations (0.1 M). With increasing pH, nonanuclear species are formed.[51] It was only very recently that the first nonanuclear bismuth-oxo-hydroxo cation was isolated, namely $[Bi_9(\mu_3\text{-}O)_8(\mu_3\text{-}OH)_6]^{5+}$.[52] The basic building unit is described as a $[Bi_4(\mu_3\text{-}O)_2(\mu_3\text{-}OH)_4]$ subunit, which is similar to the basic structural motif of $[Bi_4(\mu_3\text{-}O)_2(OSiEt_3)_8]$ (**5**). Interestingly, a hexanuclear $\{Bi_6\}$ motif of type **A** is not observed. Instead, three edge-/corner-sharing $\{Bi_5\}$ units constitute the molecular framework. The pentanuclear $\{Bi_5\}$ unit is derived from the $\{Bi_6\}$ unit **A** by removal of one bismuth atom. Similar pentanuclear metal-oxo fragments of the type $\{Bi_{5-x}Na_x\}$ are observed in $[Bi_{10}Na_5O_7(OH)_6(OSiMe_3)_{15}]$,[40] $[Bi_{15}Na_3O_{18}(OSiMe_3)_{12}]$[40] and $[Bi_{18}Na_4O_{20}(OSiMe_3)_{18}]$ (**2**). Notably, the latter contains a structural fragment of the type $[Bi_8Na(\mu_3\text{-}O)_{10}(\mu_3\text{-}OSiMe_3)_4]$ (Figure S3 in the Supporting Information), which is closely related to the bismuth-oxo framework of $[Bi_9(\mu_3\text{-}O)_8(\mu_3\text{-}OR)_6]^{5+}$ (R = H, Et).[52]

The bismuth-rich silanolates reported here might be described in terms of assemblies of the $\{Bi_6\}$ unit **A**. Thus, four $\{Bi_6\}$ units (**A**) are observed in the structures of compounds **7** and **8**, six in $[Bi_{22}O_{26}(OSiMe_2tBu)_{14}]$ (**9**) (Figure 13), ten in $[Bi_{33}NaO_{38}(OSiMe_3)_{24}]$ (**3**) and 20 in $[Bi_{50}Na_2O_{64}(OH)_2(OSiMe_3)_{22}]$ (**4**). The octahedral $\{Bi_6\}$ units of type **A** are assembled through their Bi–Bi edges to give the final bismuth-oxo cluster core. A correlation of the bismuth-oxo cluster size with the number of units **A** is shown in Figure 14.

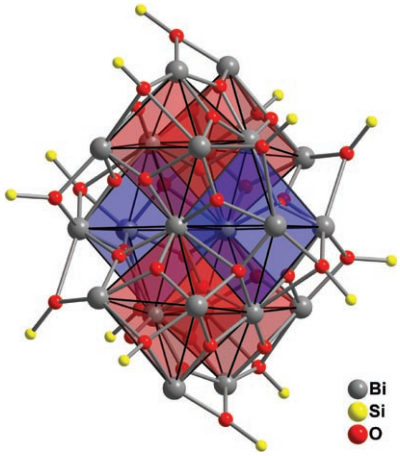

Figure 13. View of the basic structural motif in $[Bi_{22}O_{26}(OSiMe_2tBu)_{14}]$ (**9**).[38] The octahedral $\{Bi_6\}$ units **A** are highlighted in red and blue. Carbon atoms are omitted.

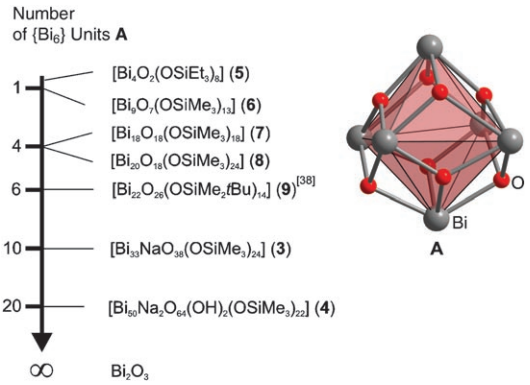

Figure 14. Correlation of the number of $\{Bi_6\}$ units **A** and the size of metal-oxo clusters. The octahedral $\{Bi_6\}$ unit **A** is highlighted in red. In **3** and **4**, there is partial substitution of bismuth atoms by sodium atoms; in $\beta\text{-}Bi_2O_3$ and $\delta\text{-}Bi_2O_3$ only three-quarters of the tetrahedral voids of the bismuth atom sublattice are occupied by oxygen atoms.

Building up an infinite structure based on the $\{Bi_6\}$ units (**A**) results in an arrangement of bismuth atoms that is close to an *fcc* structure. Similar structures have been described for bismuth compounds such as tetragonal $\beta\text{-}Bi_2O_3$ and cubic $\delta\text{-}Bi_2O_3$, both of which can be deduced from the CaF_2 structure by assuming a defect oxygen sublattice. However, in contrast to $\beta\text{-}Bi_2O_3$ and $\delta\text{-}Bi_2O_3$, in the bismuth-oxo clusters **3**, **4** and **6**–**9** all tetrahedral voids are occupied by oxygen atoms and in the sodium-containing compounds even some of the octahedral voids are occupied. It is likely that similar "defects" will occur in the solid-state structures of heterometallic bismuth compounds that are prepared starting from sodium metalates. The electronic properties of such "defect" compounds might be different from those of

the pure material. Recently, it was reported that the photocatalytic activity of monoclinic $BiVO_4$ prepared from sodium vanadate and bismuth nitrate depends on the synthetic procedure used (wet chemical route vs solid-state reaction).[53] It seems likely that different degrees of substitution of bismuth atoms by sodium atoms are responsible for the changes in electronic properties rather than the synthetic procedure used.

The most prominent BiO_n coordination polyhedron observed within the bismuth-oxo clusters is the BiO_4X (X = lone pair) pseudo-trigonal bipyramid with Bi–O bond lengths in the range 2.0–2.5 Å. Additional secondary Bi–O bonds often complete the coordination sphere at the bismuth atom and cause deviations from the ideal polyhedron. This bonding situation is closest to that found in β-Bi_2O_3. In the latter, the bismuth atom shows pseudo-trigonal bipyramidal coordination with Bi–O bond lengths of 2.096(4), 2.128(7), 2.253(7) and 2.463(7) Å.[12]

To the best of our knowledge, examples of a series of structurally closely related compounds formed along the hydrolysis pathway of metal siloxides and even alkoxides are rare. The most extensively studied compounds are those of Group IV. Several titanium-oxo alkoxides have been fully characterised,[54] in which the predominant coordination number of the titanium atoms within the metal-oxo clusters is six. The large oxygen atoms play a structure-directing role. In contrast, the hydrolysis/condensation process of bismuth silanolates is controlled by the large bismuth atoms, which leads to assembly in an *fcc* structure. The oxygen atoms occupy the corresponding voids. The coordination geometries are predominantly pseudo-tetrahedral, pseudo-trigonal bipyramidal and pseudo-octahedral, with additional bismuth–oxygen distances being significantly less than the sum of the van der Waals radii (r_{vdW}(O) 1.50 Å, r_{vdW}(Bi) 2.40 Å).[55] The lone pair on the bismuth atom causes strong distortions from ideal coordination geometries.

Conclusion

We have shown herein that hydrolysis of bismuth silanolates proceeds via polynuclear bismuth-oxo clusters. Eight bismuth-oxo silanolates of different sizes have been structurally characterised, which might be regarded as molecular models for the hydrolysis/condensation process of bismuth silanolates. The results are also likely to be of relevance to the polycondensation of bismuth compounds in general. The smallest molecule, $[Bi_4O_2(OSiEt_3)_8]$ (**5**), contains four bismuth atoms, while the largest, $[Bi_{50}Na_2O_{64}(OH)_2(OSiMe_3)_{22}]$ (**4**), contains 50 bismuth atoms. The predominant structural motif is the hexanuclear $[Bi_6O_8]^{2+}$ fragment, referred to as $\{Bi_6\}$ unit **A**. The assembly of these octahedral $\{Bi_6\}$ units (**A**) through their Bi–Bi edges results in a nearly *fcc* packing of the bismuth atoms. The oxygen atoms mainly occupy the tetrahedral voids to give a molecular structure that might be regarded as a "cut-out" of the solid-state structure of β-Bi_2O_3 with an excess of oxygen in the tetrahedral voids.

Hydrolysis of bismuth silanolates using an excess of water gives $[Bi_nO_x(OH)_y(OSiR_3)_z]$. Thermolysis of the latter has been shown to yield bismuth silicates such as $Bi_{12}SiO_{20}$ and $Bi_4Si_3O_{12}$, and bismuth oxide (α-Bi_2O_3 and β-Bi_2O_3), depending on the substituent R and the reaction conditions. Characterisation of the unprecedented $[Bi_{33}NaO_{38}(OSiMe_3)_{24}]$ (**3**) demonstrates that substitution of single bismuth atoms by sodium atoms is possible. The general motif of the *fcc* packing of the metal atoms is only slightly disturbed, but the substitution results in a change in the number and the positions of the oxygen atoms. It might be anticipated that in comparison with the parent bismuth oxide the electronic structure of such "defect" materials may be modified without an obvious change to the basic solid-state structure. This should be considered when bismuth oxide-based materials are prepared from sodium-containing precursors.

The control of the growth process of homo- and heterometallic metal-oxo particles is still challenging. The results presented here contribute to the fundamental understanding of this process. It has been shown that partial hydrolysis of bismuth silanolates offers a mild synthetic route to tailor-made bismuth-oxo clusters with dimensions in the nanometer range. In addition, the large bismuth-oxo clusters are embedded in a silanolate matrix, which offers the possibility of introducing further functionality at their periphery by exchange reactions with functionalised ligands.

Experimental Section

General procedures and instrumentation: All manipulations were performed under inert conditions using the Schlenk technique and an argon atmosphere. Solvents were distilled from appropriate drying agents prior to use. Elemental analyses were performed on a LECO-CHN analyzer. The DTA-TG measurements were performed at a heating rate of 6 °C min^{-1} to a maximum temperature of 750 °C in an atmosphere of flowing argon using Al_2O_3 as a reference material. The residues were examined by powder X-ray diffraction using a Phillips PW1050/25 diffractometer. ^{1}H and ^{29}Si NMR spectra were recorded from samples in [D$_8$]toluene at 400.13 MHz and 59.6 MHz, respectively. Chemical shifts δ are given in ppm and were referenced against Me_4Si. IR spectra were recorded from samples as Nujol mulls and absorption bands assigned to the compounds in the range 400–1400 cm^{-1} are listed. Celite (Fluka) and sodium silanolate (Aldrich) were dried in vacuo at 120 °C prior to use. Bismuth trichloride (Lancaster) was heated at reflux in thionyl chloride, washed with pentane and dried in vacuo. Triethylsilanol (ABCR) was used as received. $[Bi(OtBu)_3]$,[28] $[Bi(OSiR_3)_3]$ (R = Me, Et, *i*Pr),[35] and $[Bi_{22}O_{26}(OSiMe_2tBu)_{14}]$[38] were prepared according to literature procedures.

Synthesis

Hydrolysis of bismuth silanolates [Bi(OSiR$_2$R′)$_3$] (R = R′ = Me, Et, iPr; R = Me, R′ = tBu)—typical procedure: A solution of H_2O in *i*PrOH (12.3 mL, c = 5.55 mol L^{-1}) was slowly added to a solution of $[Bi(OSiMe_3)_3]$ (1.62 g, 3.40 mmol) in benzene (5 mL). The resulting suspension was stirred at room temperature for 20 min and then the solvent was evaporated in vacuo at 30 °C to leave an amorphous residue. The IR spectrum of the residue was indicative of partial hydrolysis. Thermolysis was carried out at a heating rate of 6 °C min^{-1} to a maximum temperature of 750 °C in an atmosphere of flowing argon. The residue was analysed by powder X-ray diffraction and the carbon content was determined. $[Bi(OSiMe_3)_3]$ gave a mixture of $Bi_{12}SiO_{20}$ (JCPDS No. 80-0627) and some $Bi_4Si_3O_{12}$ (JCPDS No. 76-1726). $[Bi(OSiEt_3)_3]$, $[Bi(OSiiPr_3)_3]$ and [Bi(O-

$SiMe_2tBu)_3$] gave $Bi_{12}SiO_{20}$. Heat treatment of the hydrolysis product of [$Bi(OSiEt_3)_3$] at 150 °C in vacuo for 4 h prior to thermolysis gave α-Bi_2O_3 (JCPDS No. 71-2274) as the final material after calcination at 750 °C. The carbon content was below the detection limit for all samples.

*Synthesis of [$Bi_{18}Na_4O_{20}(OSiMe_3)_{18}$] (**2**), [$Bi_{33}NaO_{38}(OSiMe_3)_{24}$]·3 C_7H_8 (**3**·3 C_7H_8) and [$Bi_{50}Na_2O_{64}(OH)_2(OSiMe_3)_{22}$]·2 C_7H_8·2 H_2O (**4**·2 C_7H_8·2 H_2O)*: In an attempt to prepare [$Bi(OSiMe_3)_3$] by a metathesis reaction, single crystals of the heterobimetallic compounds [$Bi_2Na_4O(OSiMe_3)_8$] (**1**),[40] [$Bi_{18}Na_4O_{20}(OSiMe_3)_{18}$] (**2**), [$Bi_{33}NaO_{38}(OSiMe_3)_{24}$] (**3**) and [$Bi_{50}Na_2O_{64}(OH)_2(OSiMe_3)_{22}$] (**4**) were obtained. These have been characterised by single-crystal X-ray diffraction analysis. $NaOSiMe_3$ (12.01 g, 107.1 mmol) was added in small portions to a suspension of $BiCl_3$ (11.26 g, 35.7 mmol) in THF (80 mL) at room temperature. The suspension turned yellow upon stirring at room temperature overnight. The THF was removed in vacuo and the solid residue was suspended in toluene (100 mL). The solid material was removed by centrifugation under inert conditions. The ^{29}Si NMR spectrum of the remaining crude reaction mixture in toluene (D_2O capillary) showed only one signal at δ = 7.4 ppm, attributable to $Me_3SiOSiMe_3$. The solution was concentrated to a volume of approximately 25 mL and benzene (25 mL) was added. After several days at 4 °C, single crystals were obtained, which by visual inspection under a microscope appeared to be a mixture. The presence of three different crystalline compounds was confirmed by single-crystal X-ray diffraction analysis: [$Bi_2Na_4O(OSiMe_3)_8$] (**1**),[40] [$Bi_{18}Na_4O_{20}(OSiMe_3)_{18}$] (**2**) and [$Bi_{33}NaO_{38}(OSiMe_3)_{24}$]·3 C_7H_8 (**3**·3 C_7H_8). A mixture of single crystals of [$Bi_2Na_4O(OSiMe_3)_8$] (**1**) and [$Bi_{50}Na_2O_{64}(OH)_2(OSiMe_3)_{22}$]·2 C_7H_8·2 H_2O (**4**·2 C_7H_8·2 H_2O) was obtained from a similar experiment after the solution had been kept for several months at 4 °C. The heterometallic bismuth-oxo silanolates are extremely moisture-sensitive and were mounted on the diffractometer by the oil-drop technique immediately after removal from the crystallisation vessel.

*Synthesis of [$Bi_4O_2(OSiEt_3)_8$] (**5**)*: A solution of Et_3SiOH (8.30 g, 63 mmol) in toluene (50 mL) was added dropwise to a solution of [$Bi(OtBu)_3$] (9.00 g, 21 mmol) in toluene (70 mL) at room temperature. The cloudy solution was filtered through Celite and all volatiles were removed in vacuo at 40 °C to give liquid [$Bi(OSiEt_3)_3$] (11.98 g, 95 %). The bismuth silanolate was dissolved in toluene and the solution was exposed to air moisture for 5 min. The solvent was partially removed in vacuo to give a concentrated solution. Crystallisation at 4 °C gave colourless crystals (1.52 g, 15 %) of [$Bi_4O_2(OSiEt_3)_8$] (**5**) with a melting point of 76 °C. After the crystals had been isolated, a second crop of single crystals was observed. Alternatively, single crystals were obtained upon slow evaporation of the solvent. ^1H NMR (C_7D_8): δ = 0.69 (q, J = 7.8 Hz, 2H; CH_2), 1.09 ppm (t, J = 7.8 Hz, 3H; CH_3); IR (Nujol): $\tilde{\nu}$ = 1414 (w), 1237 (w), 1015 (m), 974 (w), 954 (vw), 878 (s), 846 (w), 828 (w), 736 (s), 550 cm^{-1} (m); elemental analysis calcd (%) for $C_{48}H_{120}Bi_4O_{10}Si_8$ (**5**) (1918.1 $g\,mol^{-1}$): C 30.1, H 6.3; found: C 29.4, H 6.1.

*Synthesis of [$Bi_9O_7(OSiMe_3)_{13}$]·0.5 C_7H_8 (**6**·0.5 C_7H_8)*: The bismuth silanolate [$Bi(OSiMe_3)_3$] (230 mg, 0.48 mmol) was dissolved in toluene (10 mL). The solution was exposed to air moisture for 5 min and the solvent was almost completely removed. Crystallisation at 4 °C quantitatively afforded colourless single crystals of [$Bi_9O_7(OSiMe_3)_{13}$]·0.5 C_7H_8 (**6**·0.5 C_7H_8) with m.p. 210 °C (decomp) for a dried sample. IR (Nujol): $\tilde{\nu}$ = 1403 (w), 1294 (w), 1258 (m), 1245 (m), 1155 (w), 934 (s), 909 (s), 832 (s), 723 (w), 676 (w), 501 cm^{-1} (m); elemental analysis calcd (%) for $C_{39}H_{117}Bi_9O_{20}Si_{13}$ (**6**) (3152.3 $g\,mol^{-1}$): C 14.9, H 3.7; found: C 14.9, H 3.8.

*Synthesis of [$Bi_{18}O_{18}(OSiMe_3)_{18}$]·2 C_7H_8 (**7**·2 C_7H_8) and [$Bi_{20}O_{18}(OSiMe_3)_{24}$]·3 C_7H_8 (**8**·3 C_7H_8)*: Freshly prepared [$Bi(OSiMe_3)_3$] (15.63 g, 32.9 mmol) was suspended in toluene (15 mL) and the solid was removed by centrifugation under inert conditions. The solution was exposed to air moisture for 5 min. Crystallisation at −20 °C gave colourless single crystals of [$Bi_{20}O_{18}(OSiMe_3)_{24}$]·3 C_7H_8 (**8**·3 C_7H_8), which were isolated and dried in vacuo (1.21 g, 11 %); m.p. 211 °C (decomp). After the toluene solvate **8**·3 C_7H_8 had been isolated, a second crop of single crystals was obtained at 4 °C. Single-crystal X-ray diffraction analyses of this second crop showed it to consist of a mixture of **8**·3 C_7H_8 and **7**·2 C_7H_8. The supernatant solution was removed to leave a suspension of single crystals. After several weeks, single-crystal X-ray diffraction analysis of eight crystals was indicative of a pure fraction of **7**·2 C_7H_8, which was isolated and dried in vacuo (0.81 g, 8 %); m.p. 204 °C (decomp).

Compound 7: IR (Nujol): $\tilde{\nu}$ = 1453 (sh), 1408 (w), 1360 (sh), 1333 (w), 1301 (w), 1257 (m), 1244 (m), 954 (m), 909 (s), 831 (s), 742 (m), 620 (w), 564 (m, br), 540 (m), 498 (w), 478 (w), 464 (w), 427 (m), 405 cm^{-1} (brs); elemental analysis calcd (%) for $C_{54}H_{162}Bi_{18}O_{36}Si_{18}$ (5655.1 $g\,mol^{-1}$): C 11.5, H 2.9; found: C 11.4, H 2.8.

Compound 8: IR (Nujol): $\tilde{\nu}$ = 1362 (w), 1343 (w), 1293 (m), 1258 (s), 1245 (s), 956 (s), 913 (s, br), 830 (s), 742 (s), 676 (m), 620 (w), 599 (sh), 570 (s), 536 (s), 496 cm^{-1} (m); elemental analysis calcd (%) for $C_{72}H_{216}Bi_{20}O_{42}Si_{24}$ (6729.3 $g\,mol^{-1}$): C 13.1, H 3.3; found: C 14.0, H 3.3.

Structure determination: Intensity data for the colourless crystals were collected on a Nonius KappaCCD diffractometer with graphite-monochromated $Mo_{K\alpha}$ radiation. The structures were solved by direct methods using SHELXS97[56] and successive difference Fourier syntheses. Refinement was carried out by full-matrix least-squares methods using SHELXL97.[57] An absorption correction was applied with a multiscan method using SCALEPACK.[58] The figures were created with SHELXTL[59] and DIAMOND (release 2.1e, 2001). Selected crystallographic data are presented in Tables 1 and 2. Further details on the data collection and refinement are given in the Supporting Information.

CCDC-278713 (**2**), -278707 (**3**·3 C_7H_8), -278712 (**4**·2 C_7H_8·2 H_2O), -278711 (**5**), -278710 (**6**·0.5 C_7H_8), -278709 (**7**·2 C_7H_8) and -278708 (**8**·3 C_7H_8) contain the supplementary crystallographic data for this paper. These data can be obtained free of charge from the Cambridge Crystallographic Data Centre via www.ccdc.cam.ac.uk/data_request/cif.

Acknowledgements

We acknowledge the Deutsche Forschungsgemeinschaft, the Fonds der Chemischen Industrie and the Fachbereich Chemie der Universität Dortmund for financial support. S.P. is grateful to the Department of Chemistry at the University of Joensuu (Finland) and the foundation of Heikki and Hilma Honkanen for financial support as well as for receipt of an ERASMUS grant. We thank Professor Dr. K. Jurkschat for support of this work and fruitful discussions.

[1] B. H. Park, B. S. Kang, S. D. Bu, T. W. Noh, J. Lee, W. Jo, *Nature* **1999**, *401*, 682–684.
[2] M. Schuisky, K. Kukli, M. Ritala, A. Harsta, M. Leskelä, *Chem. Vap. Deposition* **2000**, *6*, 139–145.
[3] a) W. F. Su, Y. T. Lu, *Mater. Chem. Phys.* **2003**, *80*, 632–637; b) Y. Kageyama, T. Yoshida, Y. Mitsushima, K. Suzuki, K. Kato, *Integr. Ferroelectr.* **2001**, *36*, 173–181.
[4] J. H. Thurston, K. H. Whitmire, *Inorg. Chem.* **2003**, *42*, 2014–2023.
[5] a) C. A. Paz de Araujo, J. D. Cuchiaro, L. D. McMillan, M. C. Scott, J. F. Scott, *Nature* **1995**, *374*, 627–629; b) M. L. Calzada, R. Jimenez, A. Gonzalez, J. Garcia-Lopez, D. Leinen, E. Rodriguez-Castellon, *Chem. Mater.* **2005**, *17*, 1441–1449; c) Y. Tsunoda, W. Sugimoto, Y. Sugahara, *Chem. Mater.* **2003**, *15*, 632–635.
[6] a) C. Limberg, *Angew. Chem.* **2003**, *115*, 6112–6136; *Angew. Chem. Int. Ed.* **2003**, *42*, 5932–5954; b) R. K. Grasselli, J. D. Burrington, *Adv. Catal.* **1981**, *30*, 133–163; c) A. Castro, P. Begue, B. Jimenez, J. Ricote, R. Jimenez, J. Galy, *Chem. Mater.* **2003**, *15*, 3395–3401; d) A. M. Beale, G. Sankar, *Chem. Mater.* **2003**, *15*, 146–153.
[7] a) C. Limberg, M. Hunger, W. Habicht, E. Kaifer, *Inorg. Chem.* **2002**, *41*, 3359–3365; b) M. Hunger, C. Limberg, P. Kircher, *Angew. Chem.* **1999**, *111*, 1171–1174; *Angew. Chem. Int. Ed.* **1999**, *38*, 1105–1108.
[8] a) J. H. Thurston, T. O. Ely, D. Trahan, K. H. Whitmire, *Chem. Mater.* **2003**, *15*, 4407–4416; b) *High Performance Pigments* (Ed.: H. M. Smith), Wiley-VCH, Weinheim, **2001**.
[9] J. W. Pell, K. M. Delak, H. C. zur Loye, *Chem. Mater.* **1998**, *10*, 1764–1770.

[10] a) J. Wang, J. B. Neaton, H. Zheng, V. Nagarajan, S. B. Ogale, B. Liu, D. Viehland, V. Vaithyanathan, D. G. Schlom, U. V. Waghmare, N. A. Spaldin, K. M. Rabe, M. Wuttig, R. Ramesh, *Science* **2003**, *299*, 1719–1722; b) T. J. Park, Y. B. Mao, S. S. Wong, *Chem. Commun.* **2004**, 2708–2709; c) T.-J. Park, G. C. Papaefthymiou, A. R. Moodenbaugh, Y. Mao, S. S. Wong, *J. Mater. Chem.* **2005**, *15*, 2099–2105.

[11] a) G. Gattow, H. Schröder, *Z. Anorg. Allg. Chem.* **1962**, *318*, 178–189; b) G. Gattow, D. Schütze, *Z. Anorg. Allg. Chem.* **1964**, *328*, 44–68; c) H. A. Harwig, J. W. Weenk, *Z. Anorg. Allg. Chem.* **1978**, *444*, 167–177; d) H. A. Harwig, *Z. Anorg. Allg. Chem.* **1978**, *444*, 151–166; e) H. A. Harwig, A. G. Gerards, *Thermochim. Acta* **1979**, *28*, 121–131; f) O. Monnereau, L. Tortet, P. Llewellyn, F. Rouquerol, G. Vacquier, *Solid State Ionics* **2003**, *157*, 163–169; g) G. K. Moiseev, N. A. Vatolin, N. V. Belousova, *J. Therm. Anal. Calorim.* **2000**, *61*, 289–303; h) V. N. Denisov, A. N. Ivlev, A. S. Lipin, B. N. Mavrin, V. G. Orlov, *J. Phys. Condens. Matter* **1997**, *9*, 4967–4978; i) S. F. Radaev, V. I. Simonov, Y. F. Kargin, *Acta Crystallogr. Sect. B* **1992**, *48*, 604–609; j) A. Watanabe, *Solid State Ionics* **1990**, *40/41*, 889–892.

[12] S. K. Blower, C. Greaves, *Acta Crystallogr. Sect. C* **1988**, *44*, 587–589.

[13] a) J. A. Switzer, M. G. Shumsky, E. W. Bohannan, *Science* **1999**, *284*, 293–296; b) L. Leontie, M. Caraman, M. Alexe, C. Harnagea, *Surf. Sci.* **2002**, *507*, 480–485; c) V. V. Killedar, C. H. Bhosale, C. D. Lokhande, *Turk. J. Phys.* **1998**, *22*, 825–830; d) L. Leontie, M. Caraman, G. I. Rusu, *J. Optoelectron. Adv. Mater.* **2000**, *2*, 385–389; e) L. Leontie, M. Caraman, M. Delibas, G. I. Rusu, *Mater. Res. Bull.* **2001**, *36*, 1629–1637; f) J. George, B. Pradeep, K. S. Joseph, *Phys. Status Solidi A* **1987**, *103*, 607–612; g) H. Gobrecht, S. Seeck, H. E. Bergt, A. Martens, K. Kossmann, *Phys. Stat. Sol.* **1969**, *34*, 569–576; h) H. Gobrecht, S. Seeck, H. E. Bergt, A. Martens, K. Kossmann, *Phys. Stat. Sol.* **1969**, *33*, 599–606; i) A. A. Agasiev, A. K. Zeinally, S. J. Alekperov, Y. Y. Guseinov, *Mater. Res. Bull.* **1986**, *21*, 765–771.

[14] S. W. Kang, S. W. Rhee, *Thin Solid Films* **2004**, *468*, 79–83.

[15] a) W. T. Dong, C. S. Zhu, *J. Phys. Chem. Solids* **2003**, *64*, 265–271; b) B. L. Yu, C. S. Zhu, F. X. Gan, *J. Appl. Phys.* **1997**, *82*, 4532–4537.

[16] a) F. Gao, Q. Y. Lu, S. Komarneni, *Chem. Commun.* **2005**, 531–533; b) J. W. Wang, X. Wang, C. Peng, Y. D. Li, *Inorg. Chem.* **2004**, *43*, 7552–7556; c) B. J. Yang, M. S. Mo, H. M. Hu, C. Li, X. G. Yang, Q. W. Li, Y. T. Qian, *Eur. J. Inorg. Chem.* **2004**, 1785–1787; d) C. C. Huang, I. C. Leu, K. Z. Fung, *Electrochem. Solid-State Lett.* **2005**, *8*, A204–A206.

[17] P. A. Williams, A. C. Jones, M. J. Crosbie, P. J. Wright, J. F. Bickley, A. Steiner, H. O. Davies, T. J. Leedham, G. W. Critchlow, *Chem. Vap. Deposition* **2001**, *7*, 205–209.

[18] a) M. Vehkamaki, T. Hatanpaa, M. Ritala, M. Leskelä, *J. Mater. Chem.* **2004**, *14*, 3191–3197; b) C. Bedoya, G. G. Condorelli, G. Anastasi, A. Baeri, F. Scerra, I. L. Fragala, J. G. Lisoni, D. Wouters, *Chem. Mater.* **2004**, *16*, 3176–3183; c) A. Cabot, A. Marsal, J. Arbiol, J. R. Morante, *Sens. Actuators B* **2004**, *99*, 74–89; d) J. Y. Hyeon, M. Lisker, M. Silinskas, E. Burte, F. T. Edelmann, *Chem. Vap. Deposition* **2005**, *11*, 213–218; e) H. Funakubo, K. Ishikawa, T. Watanabe, M. Mitsuya, N. Nukaga, *Adv. Mater. Opt. Electron.* **2000**, *10*, 193–200.

[19] a) F. Soares-Carvalho, P. Thomas, J. P. Mercurio, B. Frit, S. Parola, *J. Sol-Gel Sci. Technol.* **1997**, *8*, 759–763; b) E. P. Turevskaya, V. B. Bergo, M. I. Yanovskaya, N. Y. Turova, *Zh. Neorg. Khim.* **1996**, *41*, 721–725; c) K. A. Vorotilov, M. I. Yanovskaya, E. P. Turevskaya, A. S. Sigov, *J. Sol-Gel Sci. Technol.* **1999**, *16*, 109–118; d) E. P. Turevskaya, V. B. Bergo, K. A. Vorotilov, A. S. Sigov, D. Benlian, *J. Sol-Gel Sci. Technol.* **1998**, *13*, 889–893; e) S. Parola, R. Papiernik, L. G. Hubert-Pfalzgraf, S. Jagner, M. Hakansson, *J. Chem. Soc. Dalton Trans.* **1997**, 4631–4635; f) Y. T. Kim, C. Hwang, H. K. Chae, Y. K. Lee, W. I. Lee, Y. W. Dong, H. Yun, *J. Sol-Gel Sci. Technol.* **2000**, *19*, 301–304; g) Y. Kim, H. K. Chae, K. S. Lee, W. I. Lee, *J. Mater. Chem.* **1998**, *8*, 2317–2319; h) K. Kato, C. Zheng, J. M. Finder, S. K. Dey, Y. Torii, *J. Am. Ceram. Soc.* **1998**, *81*, 1869–1875; i) M. L. Calzada, A. Gonzalez, J. Garcia-Lopez, R. Jimenez, *Chem. Mater.* **2003**, *15*, 4775–4783.

[20] J. H. Thurston, K. H. Whitmire, *Inorg. Chem.* **2002**, *41*, 4194–4205.

[21] L. G. Hubert-Pfalzgraf, *J. Mater. Chem.* **2004**, *14*, 3113–3123.

[22] a) K. H. Whitmire, *Chemtracts: Inorg. Chem.* **1995**, *7*, 167–181; b) J. H. Thurston, D. Trahan, T. Ould-Ely, K. H. Whitmire, *Inorg. Chem.* **2004**, *43*, 3299–3305; c) R. E. Bachman, K. H. Whitmire, J. H. Thurston, A. Gulea, O. Stavila, V. Stavila, *Inorg. Chim. Acta* **2003**, *346*, 249–255; d) S. Parola, R. Papiernik, L. G. Hubert-Pfalzgraf, C. Bois, *J. Chem. Soc. Dalton Trans.* **1998**, 737–739; e) M. Hunger, C. Limberg, P. Kircher, *Organometallics* **2000**, *19*, 1044–1050; f) J. W. Pell, W. C. Davis, H. C. zur Loye, *Inorg. Chem.* **1996**, *35*, 5754–5755; g) E. V. Dikarev, H. L. Zhang, B. Li, *J. Am. Chem. Soc.* **2005**, *127*, 6156–6157; h) D. A. Bayot, M. M. Devillers, *Chem. Mater.* **2004**, *16*, 5401–5407.

[23] K. H. Whitmire, S. Hoppe, O. Sydora, J. L. Jolas, C. M. Jones, *Inorg. Chem.* **2000**, *39*, 85–97.

[24] J. H. Thurston, A. Kumar, C. Hofmann, K. H. Whitmire, *Inorg. Chem.* **2004**, *43*, 8427–8436.

[25] T. J. Boyle, D. M. Pedrotty, B. Scott, J. W. Ziller, *Polyhedron* **1998**, *17*, 1959–1974.

[26] M. Veith, E.-C. Yu, V. Huch, *Chem. Eur. J.* **1995**, *1*, 26–32.

[27] a) R. C. Mehrotra, A. K. Rai, *Indian J. Chem.* **1966**, *4*, 537; b) M. Wieber, U. Baudis, *Z. Anorg. Allg. Chem.* **1976**, *423*, 47–52; c) C. M. Jones, M. D. Burkart, R. E. Bachman, D. L. Serra, S. J. Hwu, K. H. Whitmire, *Inorg. Chem.* **1993**, *32*, 5136–5144; d) C. M. Jones, M. D. Burkart, K. H. Whitmire, *Angew. Chem.* **1992**, *104*, 466–467; *Angew. Chem. Int. Ed. Engl.* **1992**, *31*, 451–452; e) T. A. Hanna, G. Keitany, C. Ibarra, R. D. Sommer, A. L. Rheingold, *Polyhedron* **2001**, *20*, 2451–2455; f) M. A. Matchett, M. Y. Chiang, W. E. Buhro, *Inorg. Chem.* **1990**, *29*, 358–360; g) F. Reifler, H. R. Oswald, R. A. Gubser, C. Baerlocher, A. Reller, *Solid State Ionics* **1996**, *84*, 283–291; h) W. A. Herrmann, N. W. Huber, R. Anwander, T. Priermeier, *Chem. Ber.* **1993**, *126*, 1127–1130.

[28] W. J. Evans, J. J. H. Hain, J. W. Ziller, *J. Chem. Soc. Chem. Commun.* **1989**, 1628–1629.

[29] V. G. Kessler, N. Y. Turova, E. P. Turevskaya, *Inorg. Chem. Commun.* **2002**, *5*, 549–551.

[30] S. Parola, R. Papiernik, L. G. Hubert-Pfalzgraf, S. Jagner, M. Hakansson, *J. Chem. Soc. Dalton Trans.* **1997**, 4631–4635.

[31] C. M. Jones, M. D. Burkart, K. H. Whitmire, *J. Chem. Soc. Chem. Commun.* **1992**, 1638–1639.

[32] S. C. James, N. C. Norman, A. G. Orpen, M. J. Quayle, U. Weckenmann, *J. Chem. Soc. Dalton Trans.* **1996**, 4159–4161.

[33] a) D. C. Bradley, *Coord. Chem. Rev.* **1967**, *2*, 299–318; b) A. R. Barron, *Comments Inorg. Chem.* **1993**, *14*, 123–153; c) K. Folting, W. E. Streib, K. G. Caulton, O. Poncelet, L. G. Hubert-Pfalzgraf, *Polyhedron* **1991**, *10*, 1639–1646; d) A. W. Apblett, A. C. Warren, A. R. Barron, *Chem. Mater.* **1992**, *4*, 167–182.

[34] H. Schmidbaur, M. Bergfeld, *Z. Anorg. Allg. Chem.* **1968**, *363*, 84–88.

[35] S. Paalasmaa, D. Mansfeld, M. Schürmann, M. Mehring, *Z. Anorg. Allg. Chem.* **2005**, *631*, 2433–2438.

[36] M.-C. Massiani, R. Papiernik, L. G. Hubert-Pfalzgraf, J.-C. Daran, *Polyhedron* **1991**, *10*, 437–445.

[37] K. W. Terry, K. Su, T. D. Tilley, A. L. Rheingold, *Polyhedron* **1998**, *17*, 891–897.

[38] D. Mansfeld, M. Mehring, M. Schürmann, *Angew. Chem.* **2005**, *117*, 250–254; *Angew. Chem. Int. Ed.* **2005**, *44*, 245–249.

[39] D. Mansfeld, M. Mehring, M. Schürmann, *Z. Anorg. Allg. Chem.* **2004**, *630*, 1795–1797.

[40] M. Mehring, S. Paalasmaa, M. Schürmann, *Eur. J. Inorg. Chem.*, published online: November 2, 2005, DOI: 10.1002/ejic.200500636.

[41] a) F. Lazarini, *Cryst. Struct. Commun.* **1979**, *8*, 69–74; b) B. Sundvall, *Acta Chem. Scand. Ser. A* **1979**, *33*, 219–224; c) F. Lazarini, *Acta Crystallogr. Sect. B* **1979**, *35*, 448–450; d) F. Lazarini, *Acta Crystallogr. Sect. B* **1978**, *34*, 3169–3173; e) A. N. Christensen, M. A. Chevallier, J. Skibsted, B. B. Iversen, *J. Chem. Soc. Dalton Trans.* **2000**, 265–270.

[42] a) B. Sundvall, *Inorg. Chem.* **1983**, *22*, 1906–1912; b) B. Sundvall, *Acta Chem. Scand. Ser. A* **1980**, *34*, 93–98; c) B. Sundvall, *Acta Chem. Scand. Ser. A* **1974**, *28*, 1036–1037.
[43] a) E. Asato, K. Katsura, M. Mikuriya, U. Turpeinen, I. Mutikainen, J. Reedijk, *Inorg. Chem.* **1995**, *34*, 2447–2454; b) E. Asato, K. Katsura, M. Mikuriya, T. Fujii, J. Reedijk, *Chem. Lett.* **1992**, 1967–1970.
[44] B. Kugel, W. Frank, *Z. Anorg. Allg. Chem.* **2002**, *628*, 2178.
[45] J. L. Jolas, S. Hoppe, K. H. Whitmire, *Inorg. Chem.* **1997**, *36*, 3335–3340.
[46] a) X.-W. Li, J. Lorberth, K. H. Ebert, W. Massa, S. Wocadlo, *J. Organomet. Chem.* **1998**, *560*, 211–215; b) H. J. Breunig, K. H. Ebert, R. E. Schulz, M. Wieber, I. Sauer, *Z. Naturforsch. B* **1995**, *50*, 735–744.
[47] N. N. Sauer, E. Garcia, R. Ryan, *Mater. Res. Soc. Symp. Proc.* **1990**, *180*, 921–924.
[48] W. Frank, personal communication.
[49] D. Hinz-Hübner, *Z. Anorg. Allg. Chem.* **2002**, *628*, 1811–1814.
[50] N. Henry, M. Evain, P. Deniard, S. Jobic, F. Abraham, O. Mentre, *Z. Naturforsch. B* **2005**, *60*, 322–327.
[51] K.-H. Tytko, *Chem. Unserer Zeit* **1979**, *13*, 184–194.
[52] J. H. Thurston, D. C. Swenson, L. Messerle, *Chem. Commun.* **2005**, 4228–4230.
[53] a) A. Kudo, K. Omori, H. Kato, *J. Am. Chem. Soc.* **1999**, *121*, 11459–11467; b) S. Tokunaga, H. Kato, A. Kudo, *Chem. Mater.* **2001**, *13*, 4624–4628.
[54] C. F. Campana, Y. Chen, V. W. Day, W. G. Klemperer, R. A. Sparks, *J. Chem. Soc. Dalton Trans.* **1996**, 691–702.
[55] C. Silvestru, H. J. Breunig, H. Althaus, *Chem. Rev.* **1999**, *99*, 3277–3327.
[56] G. M. Sheldrick, *Acta Crystallogr. Sect. A* **1990**, *46*, 467–473.
[57] G. M. Sheldrick, SHELXL97, University of Göttingen, **1997**.
[58] Z. Otwinowski, W. Minor in *Macromolecular Crystallography, Part A, Vol. 276* (Eds.: C. W. Carter, Jr., R. M. Sweet), Academic Press, New York, **1997**, pp. 307–326.
[59] G. M. Sheldrick, *Release 5.1 Reference Manual*, Bruker AXS, Inc., Madison, Wisconsin, USA **1997**.

Received: July 20, 2005
Published online: December 6, 2005

